National Institute of Justice, Department of Justice, Office of Justice
NIJ FY 15 Research and Development in Forensic Science for Criminal Justice Purposes.
Grant Award Number 2015-DN-BX-K015

MEASURING DESICCATION: A SYSTEM USING BIOELECTRICAL IMPEDANCE ANALYSIS.

FINAL REPORT

Melissa Connor
Director, Forensic Investigation Research Station
Colorado Mesa University
1100 North Ave
Grand Junction, CO 81501
mconnor@coloradomesa.edu
970-248-1219

Eriek S. Hansen
Associate Professor of Biology
Colorado Mesa University
1100 North Ave
Grand Junction, CO 81501
erihansen@coloradomesa.edu
970-248-1562

Christiane Baigent
Forensic Investigation Research Station
Colorado Mesa University
1100 North Ave
Grand Junction, CO 81501

Grantee DUNS number:
Grantee EIN Number:

Recipient Organization:
Colorado Mesa University
1100 North Ave
Grand Junction, CO 81501

Table of Contents

Executive Summary

This project focused on addressing the estimation of postmortem interval (PMI) in an arid environment where bodies regularly desiccate. The co-principal investigators proposed two methods to achieve this: (1) a qualitative method which scores gross change by assigning a standardized total body desiccation score (TBDS), and (2) a quantitative method through bioelectrical impedance analysis (BIA).

The TBDS scale, as designed, better describes the changes observed between desiccation and skeletonization, giving a vocabulary and description of change to what is often described as a period of stasis. In addition to the descriptive aspect, it does predict ADD (PMI indice) better in desiccated remains than the TBS scale. In the course of this, a visual dictionary was created which shows photographs of the terms used in decomposition research. This can be used to help to create a standardized vocabulary and for training (Connor and Garcia 2018).

Bioelectrical impedance analysis continues to show promise as a technique for estimating the PMI. Further research is necessary to understand the sources and mechanisms of variation in the statistical models and the techniques. The incorporation of multiple PMI estimation methods into a single model shows some of the greatest promise for reducing error in PMI estimates.

Desiccation presents differently among climatic areas of the globe. The next step in the research is to examine remains outside of FIRS to see if this desiccation vocabulary is applicable to other areas of desiccation, and whether the predictive capabilities hold.

The result of this project are two significantly improved techniques for estimating PMI in desiccated remains, one of which (BIA) had never previously been developed for use on human remains. In the course of this research, the underlying mechanisms of the skeletonization of desiccated remains are much better understood than before this project, as is the variation caused by factors other than the PMI.

1.0 Statement of the Problem

Estimation of the postmortem interval (PMI) is a complex aspect of medicolegal death investigation. Probative problems are compounded by divergence from the expected trajectory of decomposition, such as seen with bodies that desiccate rather than skeletonize. The primary focus of research has been on the active decay phase, a product of autolysis, putrefaction, and insect activity, which are expected to be regionally homogeneous and linear in trajectory. In many environments, these processes lead to skeletonization. However, much less attention has been paid to the processes that occur when the trajectory of decomposition does not result in skeletonization.

Current methods to estimate PMI beyond the first few days include insect succession and progression, patterns of gross tissue change based on observer experience, and the total body score (TBS); experimental methods include the succession and progression of microbiological communities. Insects and observer experience are probably the most commonly used methods within the medicolegal community. However, observer experience is subjective and may lack the probative robusticity necessary for judicial process. Concomitantly, in environments that foster desiccation, the trajectory of oviposition and insect development may be altered or arrested by remains too desiccated for insects to colonize. The TBS (Megyesi et al. 2005) shows a high correlation with PMI (Simmons et al. 2010), but the correlation falters in advanced decay. For example, the ability to predict accumulated degree days (ADD) using TBS as described by Megyesi et al. (2005) was not accurate when the equation was used for TBS values greater than 22 in a longitudinal study in Texas (Suckling 2011). Connor and France (2013) showed similar issues in western Colorado. Forensic microbiological methods have promise (Pechel et al. 2013) but are still experimental and focus on the early period of active decay. Estimating a useful PMI is a tenuous process, estimating PMI with desiccated remains is currently inaccurate and better left undone.

In arid environments, desiccation may be sufficient to result in retention of the dermis and soft tissue structures such as viscera, facial features, hematoma, scars, and tattoos. Collectively, retention of these features appears to constitute stasis in the decomposition process. Yet, though slow, change does occur in desiccated tissue, necessitating the development of analytical models with the resolution necessary to detect subtle patterns of change. The assessment of complex biological processes necessitates the development of multifaceted models, which may be collated to detect subtle patterns of change. Toward that end, a two component modelling for the estimation of PMI was proposed and tested at Colorado Mesa University's Forensic Investigation Research Station, Whitewater, Colorado. The two components are (a) the development of a Total Body Desiccation Score (TBDS) to describe the macroscopic, qualitative trajectory of change presented throughout desiccation; and (b) bioelectrical impedance analysis (BIA), a quantitative method used to assess changes in extracellular fluid and tissue structure throughout decomposition.

a. The Total Body Desiccation Score (TBDS): The first step was to accurately describe the sequence of gross morphological change that occurs as the body desiccates. While not typically considered "active decay," significant changes present as the body stabilizes in late

stage desiccation. Eventually, most desiccated remains exposed to a dynamic outdoor environment do skeletonize. These changes should be able to be integrated into a body scoring system, such as that initiated by Megyesi and others (2005), in a total body desiccation score (TBDS), providing an ordinal-level of measurement.

At the initiation of the study, all human bodies in the FIRS outdoor facility followed the same general pattern of desiccation. Detailed observations and photographs were taken, and all were scored using the original TBS score. Under that system, a fresh body scores 3, a fully skeletonized body consisting of dry bone scores 35. Using that system, 19 bodies placed at FIRS prior to the study period retained scores of 24 (mummified tissue covering more than one half of the body in any of the three scoring areas) for significant time periods. The four remains placed over one year prior to the onset of the study had plateaued at a score of 24. Yet, as described below, there are significant changes in color, body mass, and the consistency of the skin within that year. The goal of this facet of the study was to describe those changes and integrate them into the TBDS system. The parameters set for this description system were that it be analytically robust and have low inter-observer error.

b. Bioelectrical Impedance Analysis (BIA): Since desiccation is the removal of water from the tissue, the goal was to identify a quantitative method to measure changes in extracellular fluid across the postmortem interval. Bioelectrical impedance analysis uses an alternating current at a fixed frequency to measure electrical resistance and reactance within a biological tissue circuit. Resistance measurements are based on the composition of electrolyte gradients within the extracellular fluid, while reactance measures the capacitance of the phospholipid bilayer of cell membranes. Relationships between bioelectrical properties and the PMI were demonstrated in rats (Querido 1993). The resistance of rat abdominal walls decreased inversely with postmortem interval. Similarly, an inverse relationship between extracellular impedance measurements and postmortem interval was observed using rat abdomens (Querido and Phillips 1997). The research goals were: (a) to ensure these relationships transfer to humans; (b) determine how long the body will continue to show impedance measurements; and (c) correlate these measurements with the PMI.

The authors hypothesized that the postmortem interval of human cadavers can be estimated due to quantifiable changes that occur during decomposition due to changes in cellular and tissue composition during autolysis and desiccation. The main goal was to provide improved measures of desiccation. One objective would be through an ordinal, Likert scale called a total body desiccated score. The second measure would be a ratio-level measure of the electrical changes in the tissue. Finally both these measures would be correlated with accumulated degree-days to provide an estimate of a PMI.

2.0 Project Design and Implementation

Purpose, Goals, and Objectives

The purpose of this project is to develop techniques to better estimate the PMI of desiccated human remains using collated qualitative and quantitative methodology.

Goal 1: Describe the gross morphological changes of advanced decay when desiccation progresses to skeletonization in a manner to integrate with the total body score.
Standard methods of estimating the postmortem interval emphasize the path to skeletonization and deemphasize the delay that desiccation may cause. Instead, an emphasis is placed on what is considered active decay, when gross tissue changes are occurring quickly. However, slowly, there are significant changes in desiccated tissue from the drying of the fingers noted early in decomposition, to the thin tissue layer overlaying bone that precedes skeletonization in desiccated remains. Changes in color, the appearance of the skin, the release of moisture, and the thickness of the tissue layer are some of the specifics noted to date. The authors hypothesized that these changes correlated to accumulated degree-days.

Goal 2: Develop and evaluate the use of bioelectrical impedance analysis as a method for quantifying postmortem interval
Bioelectrical impedance analysis uses electrical currents to measure resistance and reactance. Resistance measurements are based on the composition of the extracellular fluid, while reactance measures the capacitance of the cell membranes. Impedance and other bioelectrical metrics were derived from the measurements of resistance and reactance. Based on the bioelectrical properties of tissue, postmortem changes in cellular structure and the composition of the extracellular fluid can be measured using bioelectrical impedance analysis. The authors hypothesized that the PMI of human cadavers can be estimated due to quantifiable changes that occur during decomposition due to autolysis and desiccation. Relationships between bioelectrical properties and the PMI have been demonstrated in nonhuman organisms. For example, the resistance of rat abdominal walls decreased inversely with postmortem interval (Querido 1993). Similarly, Querido and Phillips (1997) observed an inverse relationship between extra-cellular impedance measurements and postmortem interval using rat abdomens. This project tested these methods on human cadavers, rather than on animal proxies.

Review of Relevant Literature

The decomposition sequence is used as a gross, relative method of establishing PMI. The decomposition sequence as generally described is a continuum divided into four or five stages grading from fresh remains to skeletonization (e.g., Payne 1965, Reed 1958, Rodriguez and Bass 1983, Micozzi 1991; Perper 1993; Gill-King 1997; Love and Marks 2003). Desiccation of remains is discussed as a natural method of preserving tissues under conditions of high temperatures, low humidity, and good ventilation.

Studies in arid areas reveal a more complex process where desiccation slows or delays decomposition, but rarely stops decomposition altogether (Parks 2011, Galloway et al. 1989; Galloway 1997). In remains where desiccation is a dominant process, decomposition may exhibit

a different pattern that includes the mummification of the superficial aspect of remains with moist decomposition ongoing below the desiccated tissue (Parks 2011, Galloway et al. 1989). Bass (1997) points out maggots avoid direct sunlight and will use the skin as "an umbrella to protect them from the sunlight" (p.187). Drying of exposed tissue tends to alter insect utilization of cadavers and frequently disrupts the serial succession that would be otherwise expected (Hall and Doisy 1993; Archer and Elgar 2003). In many cases, desiccation appears to be a detour to decomposition, as opposed to an end in itself that produces mummified remains.

Desiccated tissue certainly has the potential to last millennia, as any number of archaeological examples show. In the general region of the study area (western Colorado), prehistoric mummies are rare, but they exist (Watson 1961, McCracken et al. 1978). A mummy from Mesa Verde is associated with Basketmaker material, making it over 1300 years old. The mummy, for which Mummy Cave in Wyoming is named, was wrapped in a mountain sheepskin garment radiocarbon dated to 1,230 +/- 110 years. The majority of archaeological skeletal material in the region is skeletal (e.g., Bennet 1975, France 1988). The point being that in the study region naturally desiccated remains exist and can persist long beyond the standard forensic time frame.

The last decade has seen substantial advances in forensic taphonomy, particularly in attempts to quantify the postmortem interval (Megyesi et al. 2005; Simmons et al. 2010; Vass 2011). Desiccation is acknowledged in these schemes to varying degrees based generally on whether the author's data set includes desiccated specimens. Megyesi and others (2005) include the drying of eyes, ears, nose and mouth as part of their "early decomposition" stage, and "mummification with bone exposure less than one half the area being scored" at the end of advanced decomposition. Neither the article by Simmons and others (2010) nor the study by Vass (2011) discusses the effect of desiccation on their efforts to quantify the postmortem interval.

The total body score proposed by Megyesi and others (2005) has proven a robust (Dabbs et al. 2016) and flexible tool. The use of body scores have been specialized for a variety of situations such as charred remains (Gruenthal et al 2012) and submerged bodies (Widya et al 2012). The advantage of using specialized body scores is that descriptive data, such as that in Galloway and others (1989), is used in a more quantifiable form (i.e., ordinal-level scale) which can be statistically manipulated. By using ordinal-data, the body scores have proven a powerful tool, if not for predictive modeling, then for isolating variables which most strongly affect decomposition (e.g., Simmons et al. 2010).

Decomposition processes vary with climatic conditions as shown by research at multiple forensic research stations. For example, at the Anthropological Research Facility in Tennessee, Vass and others (1999) suggested that remains were mainly skeletal by 1287 ADD. This decomposition pattern is clearly not consistently the case in arid areas. Galloway and others (1989) suggested that in an arid area, the high temperatures and low humidity alter the reported sequences and timing of decomposition. However, they also conclude that there may be surface desiccation within two weeks and insect and carnivore activity reduce these to skeletal elements in four to six months. At the Forensic Anthropology Research Facility at Texas State University, accumulated degree-days for mummification range from 241 to 1698, with skeletonization taking from two months to more than two years (Wescott et al 2013). The University of Montana – Missoula also has a research program that is examining decomposition in a relatively arid

environment. The series of research projects completed use pigs as a surrogate for human remains (Barnes 2000, Parsons 2009, Wagster 2007, White 2013), and is also finding that desiccation occurs regularly. At the Montana site, three pigs used in research mummified within the first 10 days. The first two pigs had mummified shells in 7 and 10 days with insect activity under the shell for a few weeks thereafter (White 2013).

Closer to the study area, Connor and France (2013) examined forensic cases analyzed by anthropologist Diane France in the vicinity of the study region. They ranged from frozen, to adipocere, to mummified, to skeletonized – in a total of eight cases. The data were too few and too variable to form a pattern, but they do provide data points. One of the more interesting cases is a case from Weld County, Colorado where the remains experienced approximately 1284 ADD, and was mummified on the exposed side, but showed insect activity inside and under the mummified tissue (France, personal communication 2013). In another case, there was desiccated tissue lasting to approximately 5884 ADD. Also, in this case, there was a clear line of demarcation along the clothing line, with better preservation under the shirt, suggesting that the clothing played a role in differential decomposition, as have other studies (e.g. Dautartas 2009, Notter and Stuart 2012).

From the available data the authors were able to infer: (1) fully skeletonized remains are rare in western Colorado and other areas in the western United States and skeletonization may take long past 1280 ADD; (2) a slowing of decomposition is seen with dehydrated tissue on the top portion of the body, with active, moist decomposition occurring under this harder shell – a pattern also noted by Galloway and others (1989) and Parks (2011); and (3) clothing does play a role in differential decomposition.

These desiccation and skeletonization patterns prompted the investigation of BIA as a potential method for quantifying PMI. BIA has traditionally been used to quantify the proximate body composition (water, lipid, and lean masses) in living organisms (Van Marken Licthenbelt 2001). BIA uses four electrodes to introduce the electrical current and to measure electrical resistance and reactance. Resistance measurements are based on the composition of the extracellular fluid, while reactance measures the capacitance of the cell membranes. Impedance and other bioelectrical metrics can be derived from the measurements of resistance and reactance. Based on the bioelectrical properties of tissue, postmortem changes in cellular structure and the composition of the extracellular fluid can be measured using bioelectrical impedance analysis. Relationships between bioelectrical properties and the postmortem interval have been demonstrated in nonhuman organisms. For example, the resistance of rat abdominal walls decreased inversely with postmortem interval (Querido 1993). Similarly, Querido and Phillips (1997) observed an inverse relationship between extra-cellular impedance measurements and postmortem interval using rat abdomens.

Research Design and Methods

The Study Location

This research was performed at the Forensic Investigation Research Station (FIRS) located on the Whitewater Campus of Colorado Mesa University. FIRS is in Mesa County, Colorado. Altitude within the county ranges from about 4,300 feet along the Colorado River to 11,234 ft at Leon Peak on Grand Mesa north of the facility. In the desert area of the county – where the facility is – annual precipitation ranges from 8 to 10 inches. Summers are hot, winters are moderate and the frost-free season ranges from 100 to 125 days (Spears and Kleven 1978). FIRS is in the area of Utaline-Neiman-Lazear association of soils. These are well-drained loam soils formed in materials weathered from basalt and sandstone (Spears and Kleven 1978). Generally, the soil is alkaline and an inch of topsoil can take approximately 2,000 years to form in this area (Swift 2012). The soil map for the county shows that the facility is in an area of Billings silty clay loam (Spears and Kleven 1978). The natural vegetation is mainly saltbush, rabbit brush, Galleta and Indian ricegrass. Construction destroyed most of the vegetation in the immediate area of the facility, but saltbush was planted in the outdoor facility to assist in screening the remains from the air and from distant areas with some visibility into the fenced area. The authors are taking soil samples from the outdoor facility now, before heavy use as a decomposition facility begins and has the potential to change soil characteristics. These samples can be used as a base for later soil analysis.

FIRS includes a 2700 sq. ft. building with a classroom, a processing laboratory, a morgue cooler, and a skeletal collection storage room. The FIRS facility also includes one acre of fenced land. At 4780’ AMSL it is the highest decomposition research facility currently using human remains, the next closest being the facility in Western Carolina University at approximately 2200’ AMSL. With an average annual precipitation of less than nine inches, it is also the driest facility, with the next driest being the facility near Sam Houston University with an approximate annual precipitation of 32 inches. Grand Junction, Colorado is also a relatively sunny area, receiving approximately 70% of available sunshine. Being in an arid, high-altitude desert, FIRS has an environment unlike the other extant decomposition study centers.

A HOBO weather station, located inside the fence in the outdoor facility records temperature, humidity, rainfall, wind speed and direction, and solar radiation on an hourly basis. Standard data collection on all human remains includes regular photographs and TBS assessment.

Methods

Total Body Desiccation Score (TBDS). The study consisted of three stages: (1) a long-term observation of 40 human bodies used to develop a scoring system much of which occurred prior to the current grant; (2) scoring of 17 bodies by one individual to assess whether the observations correlate with the postmortem interval; and (3) scoring multiple bodies diachronically and synchronically to test the correlation with the post-mortem interval.

Stage 1: Long-term observation of 40 human bodies was used to develop a pilot model for scoring the trajectory of desiccation. Categories included color, bloat, moisture, desiccation, and

skeletonization. Subcategories were identified to describe both intragroup variation, and the progression of decompositional change. Subcategories were weighted with a score that increased in value as decomposition progressed, resulting in a maximum combined score (TBDS) of 100. Categorical change was compiled into a standard scoring matrix. The scores were applied to body regions following Megyesi et al (2005), defined as: (1) head/neck; (2) thorax; (3) arms; and (4) legs. The arms and legs were separated as suggested by Dabbs and others (2016).

Stage 2: Photographic packets were compiled to test the new model. In order to represent a range of seasons and postmortem intervals, a sequential data pool of 40 donors was sampled and every fifth donor was selected (n=8). Each donor was represented by monthly data points commencing on the date of deposition and ending either at the time of recovery, or at the terminus of the study (May 2016). Randomly generated numbers replaced body numbers and dates. This method produced a study cohort composed of 17 donors which yielded 112 data points; each data point represented one body and one date. To avoid hindsight bias, the second author scored each packet and the senior author analyzed the data independently. Each category (color, bloat, moisture, desiccation, and skeletonization) was independently assessed to determine degree of correlation to ADD. Subcategory scores were re-weighted to reflect changes made to the pilot scoring model and standardized for daily data collection.

Stage 3: The modified scoring matrix was introduced to daily data collection at the end of 2017. Daily data collection protocols and a photographic index were established to ensure continuity in daily data collection. All donors placed proceeding the initiation of data collection were scored daily, resulting in the diachronic scoring of 12 donors at the terminus of the study period. Additionally, a broader study cohort composed of donors presenting advanced decomposition and desiccation were scored periodically, resulting in a synchronic data set composed of 41 bodies. These data were assessed to test the model's correlation to the postmortem interval.

Bioelectrical Impedance Analysis (BIA). Over the course of the study multiple electrode types (i.e., gel pads and needles), electrode distances (i.e., variable distance and fixed distance electrodes), body segments (i.e., landmark and segmental BIA), and measurement intervals (i.e., daily and weekly) were evaluated to refine and improve the use of BIA for estimating PMI. All methods used 50 KHz 400 μA, tetrapolar BIA with distal current source electrodes and proximal current detecting electrodes. Two electrode types were used: (1) adhesive gel pads (RJL Systems; required the use of duct tape and stitches to maintain adhesion during decomposition); and (2) 0.7 mm x 38.1 mm aluminum hub hypodermic needles. Variable distance measurements used paired current source – detecting electrodes positioned 10 cm apart and the distance between detecting electrodes varied with donor stature. Fixed distance measurement did not vary with donor stature and maintained a constant 6.2 cm distance between detecting electrodes and 3.5 cm between a current source and detecting electrode. Body segments (hand-foot, hand-shoulder, and thigh-foot were isolated by positioning electrodes at anatomical landmarks on one side of the body. In contrast, segmental BIA used electrodes positioned on both hands and feet and isolated body segments using different combinations of current source and detecting

electrodes. The following combinations of electrode type, distance, body segment, and measurement interval were used in the study.

- Variable-distance, gel pad electrodes: Gel pad electrodes using anatomical landmarks to isolate body segments were positioned on one side of the body. Paired current-detector electrodes were positioned 10 cm apart at the hand and foot. Resistance, reactance, and body temperature were measured daily, given adequate staffing and weather conditions.
- Variable-distance, unilateral needle electrodes: Needle electrodes using anatomical landmarks to isolate body segments (Table 3.2) were positioned on one side of the body. Paired current-detector electrodes were positioned 10 cm apart at the hand, shoulder, hip, and foot. Resistance, reactance, and body temperature were measured daily, given adequate staffing and weather conditions.
- Variable-distance, bilateral needle electrodes: Needle electrodes positioned on both hands and feet to isolate body segments (Table 3.3). Resistance, reactance, and body temperature were measured daily, given adequate staffing and weather conditions.
- Fixed-distance: Needle electrodes positioned at the mid-humerus and mid-femur, bilaterally. Resistance, reactance, and body temperature were measured daily, given adequate staffing and weather conditions.

To estimate the PMI (i.e., ADD) a linear mixed effects modeling approach was used with the lme4 package (Bates et al. 2015) in Program R (R Core Team 2017). Linear mixed effects models were used due to the lack of independence among measurements within each body, an unbalanced design, and the ability of the model to account for variation among individual bodies that could not be characterized during model application (e.g., proximate body composition). In the reported models ADD (transformation $\log_{10}$ ADD+1) was the response variable, the fixed effects were TBS^2 and Z_{sl} (s indicates measurement in series and l indicates the impedance was standardized by the distance between electrodes), and the random effects (random intercept and slope) were Z_{sl} and donor. This model was compared to a model without TBS^2. Models were evaluated using observed versus predicted ADD with the same data used to develop the model.

Preliminary analysis indicates that donor temperature affects resistance and reactance measurements. Originally donor temperature was included in the regression models, but this approach was problematic since a temperature-based metric was used as the indice of PMI. To develop temperature correction equations for R and X, a pork roast was cooled and allowed to warm while R, X, and temperature were measured. The cooling-warming sequence was repeated at multiple stages of decomposition. Four modeling approaches were used to develop correction equations: random intercept regression, multiple regression, 2.5% correction (Querido 2000), and a percent correction based on the pork roast data. The means sum of the differences squared was used to compare the modeling approaches.

3.0 Results

Total Body Desiccation Score

Stage 1. In the observation phase, many of the early-stage changes noted by Megyesi et al (2005) were similar in the study cohort and were maintained in the scoring matrix. However, there were prominent differences in the color category. The majority of the observed differences were in the advanced stages of decomposition and subcategories were added to reflect these differences. Additionally, categories were established to reflect region specific changes in moisture and desiccation, creating a more finely grained scoring for skeletonization than in the original TBS system.

The primary categories of change were defined as: color, bloat, moisture, desiccation, and skeletonization. Subcategories were assigned as follows:

> *Color*: natural, marbling, gray/green, black/ orange, brown/orange, and parchment (Figure 3.1). Color change is not homogeneous across the decomposition event; a donor may present all defined iterations of color change, or a variable subset within. These subcategories captured prominent points within the continuum observed among the majority of remains.
>
> *Bloat*: none/fresh, slight, full bloat, and post bloat. Pre-bloat and post-bloat could usually be differentiated by the caving of tissues found in the post-bloat specimens.
>
> *Moisture*: none, purge, soil surrounding remains wet, the remains "sweating" or "glistening", and by dry remains (Figure 3.2).
>
> *Desiccation*: none, drying of edges (fingers, toes, ears, etc.). Three categories then seemed to overlap in the middle of the sequence were identified and defined as skin that presented as rawhide, skin that was crenulated, and skin presenting a rough surface termed "pebbled mosaic" (Figure 3.3). The "pebbled mosaic" appears to be a sloughing of the external epidermis where islands of raised tissue remain between the sloughed areas. The final stage in desiccation before skeletonization was a stage called "parchment" where the tissue became increasingly thin and dry, eventually mechanically breaking from wind, rain, or similar ambient variables.
>
> *Skeletonization* in Megyesi et al (2005) was broken into categories based on whether the body area score was over or under 50%. This proved too broad a category for a geographical area where it could take a year before any bone was exposed. For this project, it was changed was to four categories: (1) 0 bone exposed; (2) 1-25%, (3) 25-50%, (4) 50-75%, and (5) 75-100% of the body area exposed. This resulted in finer grained information, but a score that could still be estimated in the field (Figure 3.4)

This resource was prepared by the author(s) using Federal funds provided by the U.S. Department of Justice. Opinions or points of view expressed are those of the author(s) and do not necessarily reflect the official position or policies of the U.S. Department of Justice.

Qualitative filters: changes that either had not happened, were in the process of happening, or had occurred. One was defined for each body segment scored. They were: (1) the exposure of the maxillary dentition, (2) the visible definition of the patella, (3) the visible definition of the ribs and pelvic girdle, creating an "O" shape in the abdomen, and (4) the visible definition of the humoral head (Figure 3.5).

As these observations were being collated, a visual dictionary was created, which shows pictures for each term used in the scoring system as well as a number of terms used in decomposition research (adipocere, marbling, purging, skin slippage) (Connor and Garcia 2018). The junior author went through the pictures from the FIRS data collection and selected examples of early stage, normal and extreme versions of each condition, where appropriate. This is in draft as the senior author is still in the process of removing identifying features from the photographs, but the material is incorporated into the FIRS Technical Manual series and currently being used to train interns.

Stage 2

The five categories: color, bloat moisture, desiccation, and skeletonization were each correlated against ADD and then added together in a total body desiccation score (TBDS) and correlated with ADD (Figure 4). Of the individual categories, bloat correlated the worst with ADD (). Color and moisture had stronger correlations at higher ADD categories. The desiccation category, as defined, initially shows a solid correlation with ADD, but spreads out in the later stages (Figure 3.6).

When the same sample was compared for TBS and TBDS, both showed the same correlation (r^2=0.87), and the TBDS had a higher standard error (TBS se=.298; TBDS se=.417). However, when the later stages of decomposition were examined (TBS>20 and TBDS>50), the TBDS had a slightly higher correlation (TBS r^2=.504 and TBDS r^2=.600) and a lower standard error (TBS se=.253; TBDS se=.163), suggesting that the TBDS does provide a higher resolution for the later stages of decomposition.

Stage 3

On May 29, 2018 41 bodies that were in the outside facility at FIRS were scored using a single observer for both TBS and TBDS. The correlation co-efficient between the decomposition scales and ADD were:

$$r_{(TBDS,\ ADD)} = 0.79$$

$$r_{(TBS,\ ADD)} = 0.68$$

The ADD ranged from 590 to slightly over 21,000, but this was generally a late-stage.

The TBDS scale does predict ADD better in desiccated remains than the TBS scale. The TBDS systems performs as designed and better describes the changes seen between desiccation and skeletonization, giving a vocabulary and description of change to what is often described as a period of stasis.

However, desiccation presents differently among climatic areas of the globe. The next step in the research is to examine remains outside of FIRS to see if this vocabulary is applicable to other areas of desiccation, and whether the predictive capabilities hold.

Bioelectrical Impedance Analysis (BIA)

The length of time (ADD) BIA measurements were possible varied among the four BIA measurement approaches (Tables 3.1-3.4). The measurement methods in order from shortest to longest measurement period were variable-distance gel pad electrodes positioned at the hand-foot position, variable-distance needle electrodes positioned at anatomical landmarks, variable-distance needle electrodes using segmental techniques, and fixed-distance needle electrodes.

Variable-distance, gel pad electrodes using anatomical landmarks yielded measurements for the shortest PMI. However, Z standardized by stature showed strong correlations with ADD (Hansen et al. 2017; Table 3.1; Figure 3.7).

Variable-distance, needle electrodes using anatomical landmarks yielded measurements for the second shortest PMI. The measurement period was similar among all four body-segments. Models accounted for >90% of the variation when accounting for random effects (conditional R^2) and >70% of the variation for fixed effects (marginal R^2) excluding the shoulder-thigh body segment (Table 3.2; Figures 3.8-3.12).

Variable-distance, needle electrodes positioned on both hands and feet to isolate body segments yielded measurements for the second longest PMI. The difference in PMI is based on the positioning of the electrodes and the pattern of current sources and detecting electrodes used by the segmental equipment. Models accounted for less of the variation in the data compared to the measurement approach using anatomical landmarks (Table 3.3; Figures 3.13-3.25). The increased variation may be attributed to the increased measurement period, or due to a greater number of donors used in the models. The outdoor facility at FIRS presents a slight camber along which donors were horizontally placed, resulting in downslope orientation of one lateral half of the body. Differences in slope orientation were considered in analysis. Models for measurements on the downslope side of the body were more variable than the upslope side of the body based on model coefficient standard errors and coefficient of determinations (Table 3.3). The upslope body segments were similar in the measurement period and the amount of variation accounted for by the LMM model. The models for body segments with measurements across both sides of the body accounted for similar amount of the variation when random effects were included (conditional R^2) but accounted for less variation in the fixed effects (marginal R^2; Table 3.3).

Fixed-distance, needle electrodes positioned bilaterally at the mid-humerus and mid-femur yielded BIA measurements for the longest PMI. Similar to the variable-distance segmental approach, the downslope side of the body yielded more variable measurements than the upslope side. Models including random effects account for a higher amount of variation (conditional R^2) than the variable-distance needle electrode segmental approach, but similar to variable-distance needle electrode anatomical landmark method (Table 3.4; Figures 3.26-3.29). However, compared to the other measurement methods the fixed-distance approach did not account for as much of the variation when evaluating the model fixed effects only (marginal R^2). Compared to the other measurement methods the fixed-distance approach used the highest number of different donors.

To develop temperature correction equations for resistance and reactance measurements only a pork roast was used. No bodies in the appropriate condition (i.e. fresh, non-autopsied, presenting no trauma or significant pathology) were available when the appropriate environmental conditions occurred for cooling and warming the remains. In the comparison of correction models, multiple regression yielded the lowest mean sum of squares (Table 3.5; Figure 3.30). Further development of the models using human subjects is necessary before utilizing corrections for use in predictive models.

Conclusions

An arid environment significantly affects the decomposition trajectory away from the patterns described in the literature from elsewhere, particularly the eastern Woodlands of the United States. Changes include differences in the sequences of bloat and color. Moist decomposition can last years. A long period of stasis occurs between moist decomposition and skeletonization.

The first portion of this project described the differences in decomposition, the second tried two techniques to predict the post-mortem interval in arid environments. The TBDS scale does predict ADD better in desiccated remains than the TBS scale. It does what it was designed to do and better describes the changes seen between desiccation and skeletonization, giving a vocabulary and description of change (Connor and Garcia 2018) to what is often described as a period of stasis.

Bioelectrical impedance analysis continues to show promise as a technique for estimating the PMI. Further research is necessary to understand the sources and mechanisms of variation in the statistical models and the techniques. The incorporation of multiple PMI estimation methods into a single model shows some of the greatest promise for reducing error in PMI estimates.

References

Archer, M.S. and M.A. Elgar (2003). Effects of decomposition on carcass attendance in a guild of carrion-breeding flies. Medical and Veterinary Entomology 17: 263-271.

Barnes, S. (2000) Forensic entomological case study and comparison of burned and unburned Sus scrofa specimens in the biogeoclimatic zone of northwestern Montana. Masters' thesis, Department of Anthropology. University of Montana, Missoula, Montana.

Bass, W. M. (1997) Outdoor decomposition rates in Tennessee. In Haglund and Sorg (eds) Forensic Taphonomy: The Post-Mortem Fate of Human Remains, CRC Press. PP 181-186.

Bennett, K. A. (1975) Skeletal remains from Mesa Verde National Park, Colorado. Washington: U.S. Dept. of the Interior, National Park Service. U.S. Gov't Printing Office.

Burnham, K. P., and D. R. Anderson (2002). Model selection and multimodel inference: a practical information-theoretic approach (second edition). Springer Science+Business Media, Inc. U.S.A.

Connor, M., and D. L. France (2013). A Two-Pronged Model for Regional Taphonomic Studies: A Case Example from Mesa County, Colorado. Proceedings of the American Academy of Forensic Sciences 65th Annual Meeting, Washington, D.C.

Connor, M. and S. Garcia (2018). The Visual Dictionary for Taphonomy. FIRS Technical Manual 6. Forensic Investigation Research Station, Colorado Mesa University, Grand Junction CO. Draft.

Dabbs, G.R., M. Connor, and J. Bytheway (2016). Interobserver Reliability of the Total Body Score System for Quantifying Human Decomposition. Journal of Forensic Sciences 61(2):445-451.

Dautartas, A. M. (2009) The Effect of Various Coverings on the Rate of Human Decomposition. Master's Thesis, University of Tennessee. http://trace.tennessee. edu/utk_gadthes/69

Decker, P. (1978) Postmortem bacteriology. Bulletin of the Ayer Clinical Laboratory. New Series 4(2):2-5.

France, D. (1988) A Human Burial from Dolores County, Colorado. Bureau of Land Management Colorado Cultural Resource Series 24. Colorado State Office, Bureau of Land Management, Denver.

Galloway, A. (1997) The Process of Decomposition: A Model from the Arizona-Sonoran Desert. In Haglund and Sorg (eds) Forensic Taphonomy: The Post-Mortem Fate of Human Remains, CRC Press. PP 139-150.

Galloway, A, W Birkby, A Jones, T Henry, and B Parks. (1989). Decay Rates of Human Remains in an Arid Environment. Journal of Forensic Sciences 34(3):607-616.

Gill-King, H. (1997) Chemical and Ultrastructural Aspects of Decomposition. In Haglund and Sorg (eds) Forensic Taphonomy: The Post-Mortem Fate of Human Remains, CRC Press. PP 93-108.

Gruenthal, A., C. Moffatt, and T. Simmons (2012). Differential Decomposition Patterns in Charred Versus Un-Charred Remains. Journal of Forensic Sciences 57 (1):12-18

Haglund, William, and Marcella Sorg (1997). Method and Theory of Forensic Taphonomic Research. In Haglund and Sorg (eds) Forensic Taphonomy: The Post-Mortem Fate of Human Remains, CRC Press. PP 13-26.

Hall, R.D., and K.E. Doisy (1993). Length of time after death: Effect on attraction and oviposition or larviposition of midsummer blow flies (Diptera: Calliphoridae) and flesh flies (Diptera: Sarcophagidae) of medicolegal importance in Missouri. Annuals of the Entomological Society of America 86(5):589-593.

Love, J.C. and M.K. Marks (2003). Taphonomy and time: estimating the postmortem interval. In D.W. Steadman (ed) Hard evidence: case studies in forensic anthropology. Pearson Education, Inc. New Jersey. PP 160-175.

Mailick, M.S., J.M.F. Siccieri, and A.A. Jordao Jr. (2014) Analysis of body composition: A Critical Review of the Use of Bioelectrical Impedance analysis. International Journal of Clinical Nutrition 2(1):1-10.

Mann, R.W., W. M. Bass, and L. Meadows (1990) time since death and decomposition of the human body: Variables and observations in case and experimental field studies. Journal of Forensic Sciences 35: 103-111.

McCracken, H., W. Wedel, R. Edgar, J.H. Moss, H.E. Wright, W.M. Husted, W. Mulloy (1978). The Mummy Cave Project in Northwestern Wyoming. Buffalo Bill Historical Center, Cody, Wyoming.

Megyesi, Mary, Stephen Nawrocki, Neal Haskell (2005). Using Accumulated Degree-Days to Estimate the Postmortem Interval from Decomposed Human Remains. Journal of Forensic Sciences 50 (3): 618- 626.

Micozzi, M. (1991) Postmortem change in human and animal remains. Charles C. Thomas, Springfield, IL.

Notter, S. J. and Stuart, B.H. (2012). The effect of body coverings on the formation of adipocere in an aqueous environment. Journal of Forensic Sciences 57 (1): 120-125

This resource was prepared by the author(s) using Federal funds provided by the U.S. Department of Justice. Opinions or points of view expressed are those of the author(s) and do not necessarily reflect the official position or policies of the U.S. Department of Justice.

Parks, Connie L. (2011). A Study of the Human Decomposition Sequence in Central Texas. Journal of Forensic Sciences 56 (1): 19-22.

Parsons, Hillary Renee (2009) The Postmortem interval: A Systematic Study of Pig Decomposition in West Central Montana. Master's thesis, University of Montana, Missoula, MT.

Payne, J.A. (1965). A summer carrion study of the baby pig Sus scrofa Linnaeus. Ecology 46:592-602.

Pechal, JL, TL Crippen, ML Benbow, AM Tarone, S Dowd, JK Tomberlin. (2013). The potential use of bacterial community succession in forensics as described by high throughput metagenomic sequencing. International Journal of Legal Medicine June.

Perper, J. A. (1993) Time of Death and Changes after Death. Part I. Anatomical Considerations. In W. Spitz (ed.) Spitz and Fisher's Medicolegal Investigation of Death: Guidelines for the Application of Pathology to Crime Investigation. Third Edition. Charles C. Thomas Publisher, Springfield, IL PP. 14-49.

Querido, D. (1993). Postmortem changes in resistivity of the anterior abdominal wall during the early postmortem period in rats. Forensic Science International 60:163-177.

Querido, D. And M. R. B. Phillips. (1997). Transcellular and extracellular impedances of the intact abdomen in putrefying rat cadavers. Forensic Science International 90:185-195.

Reed, H. (1958) A study of dog carcass communities in Tennessee, with special reference to the insects. American Midland Naturalist 59:213-245.

Rodriquez, W.C. and W.M. Bass (1983) Insect activity and its relationship to decay rates of human cadavers in East Tennessee. Journal of Forensic Sciences 28:423-432.

Simmons, T., P. Cross, R Adlam, and C Moffatt. (2010). The Influence of Insects on Decomposition Rate in Buried and Surface Remains. Journal of Forensic Sciences 55(4): 889-892.

Sorg, M., J. Wren, and W. Parker (2013). Regional and micro-Environmental taphonomic variation and decomposition in northern New England. Proceedings of the American Academy of Forensic Sciences 65th Annual Meeting, Washington, D.C.

Spears, C. F. and E.V. Kleven (1978). Soil Survey of Mesa County area. Soil Conservation Service and Colorado Agricultural Experiment Station. [Washington?]: The Service.

Suckling, J.K. (2011). A Longitudinal Study on the Outdoor Human Decomposition Sequence in Central Texas. Master's Thesis, Texas State University, San Marcos, TX.

Swift, C. (2012) The Soils of Western Colorado Mesa Delta and Montrose Counties. Colorado State University Extension. Retrieved from http://www.coopext.colostate.edu/TRA/PLANTS/gvsoil.shtml

Van Marken Lichtenbelt, W. D. (2001). The use of bioelectrical impedance analysis (BIA) for estimation of body composition. Pages 161-187 in J. R. Speakman, editor. Body composition analysis of animals: a handbook of non-destructive methods. Cambridge University Press, Cambridge, United Kingdom.

Vass, AA (2011). The elusive universal post-mortem interval formula. Forensic Science International 204: 34-40.

Vass, A.A., W.M. Bass, J.D. Wolt, J.E. Foss, J.T. Ammons (1999) Time since death determination of human cadavers using soil solution. Journal of Forensic Sciences 37(5): 1236-53.

Wagster, L.B. (2007) Decomposition and the freeze-thaw process in northwest Montana: a preliminary study. Master's thesis, Department of Anthropology, University of Montana, Missoula.

Watson, D. (1961). Indians of the Mesa Verde. Mesa Verde Museum Association. Mesa Verde National Park, Colorado.

Wescott, D., M. D. Hamilton, and K. Spradley (2013) Regional Factors in Central Texas Affecting Postmortem Decomposition in Human Remains. Proceedings of the American Academy of Forensic Sciences 65th Annual Meeting, Washington, D.C.

Widya, M., C. Moffat, and T. Simmons (2012). The Formation of Early Stage Adipocere in Submerged Remains: A Preliminary Experimental Study. Journal of Forensic Sciences 57(2): 328-333.

White, T. (2013) A Forensic Entomology Study of Postmortem Changes in the Northern Rocky Mountains using Pig (Sus Scrofa) Cadavers. Master's thesis, University of Montana, Missoula, MT.

TABLES

Table 3.1. Coefficients for the quadratic regression equation $ZH=\beta0+ \beta1\cdot ADD+ \beta2\cdot ADD2+\varepsilon$ for each donor. Coefficient standard errors (S.E.) are in parentheses. Hansen et al. 2017.

Cadaver	β_0 (S.E.)	β_1 (S.E.)	β_2 (S.E.)	Degrees of freedom	F-statistic	p-value	Coefficient of determination (R^2)
A	5.1451 (0.7324)	-0.0706 (0.0148)	0.0003 (0.0001)	3, 14	14.331	<0.001	0.67
B	5.7973 (0.6986)	-0.1142 (0.0166)	0.0007 (0.0001)	3, 7	67.996	<0.001	0.95
C	4.1960 (0.6257)	-0.0770 (0.0159)	0.0005 (0.0001)	3, 5	27.440	0.002	0.92
D	4.6621 (0.7086)	-0.0913 (0.0132)	0.0005 (0.0001)	3, 9	127.988	<0.001	0.98

Table 3.2. Fixed effect coefficients from linear mixed effects model for variable-distance BIA measurements using anatomical landmarks and needle electrodes to isolate body segments.

			Fixed effects										
Body Segment	Bodies	n	Intercept	Intercept S.E.	TBS^2	TBS^2 S.E.	BIA	BIA S.E.	Marginal R^2	Conditional R^2	ADD_{max} mean	ADD_{max} minimum	ADD_{max} maximum
Hand-Foot	5	211	-90.67	62.07	1.47	0.03	24.83	39.03	0.73	0.94	546	213	874
Hand-Shoulder	5	211	-58.99	62.66	1.35	0.03	6.79	9.07	0.74	0.95	561	213	778
Shoulder-Foot	5	196	-42.95	52.01	1.31	0.03	0.77	23.30	0.73	0.95	480	213	654
Shoulder-Thigh	5	187	-27.68	54.01	1.26	0.03	-27.67	43.32	0.53	0.96	516	213	855
Thigh-Foot	5	221	-90.00	60.39	1.44	0.03	27.82	25.83	0.74	0.95	625	213	874

Table 3.3. Fixed effect coefficients from linear mixed effects model for variable-distance BIA measurements using segmental BIA and needle electrodes Asterisks (*) indicate the measurement was on the downslope side of the body, dagger (†) indicates slope was not applicable.

			Fixed effects										
Body Segment	Bodies	n	Intercept	Intercept S.E.	TBS^2	TBS^2 S.E.	BIA	BIA S.E.	Marginal R^2	Conditional R^2	ADD_{max} mean	ADD_{max} minimum	ADD_{max} maximum
Hand-Foot	12	763	-201.95	46.14	1.67	0.06	30.11	17.47	0.59	0.84	766	222	1828
Hand-Foot*	12	720	-224.14	59.87	1.84	0.08	26.66	22.07	0.47	0.70	860	223	1828
Hand-Shoulder	12	803	-241.20	41.87	1.86	0.06	19.71	5.45	0.71	0.89	854	27	1919
Hand-Shoulder*	12	727	-165.50	43.89	1.83	0.07	1.01	6.54	0.44	0.77	890	250	2125
Shoulder-Thigh	11	458	-143.49	40.81	1.75	0.07	39.92	24.08	0.46	0.86	904	26	1841
Shoulder-Thigh*	9	476	-129.10	65.72	1.82	0.07	52.38	38.62	0.31	0.95	1008	522	1820
Thigh-Foot	12	730	-198.46	55.81	1.78	0.06	33.89	6.52	0.67	0.87	961	278	2125
Thigh-Foot*	12	728	-185.30	93.96	2.02	0.07	17.06	9.88	0.36	0.80	1036	223	2054
Hand-Hand†	11	725	-195.24	54.92	1.60	0.06	19.12	17.37	0.48	0.56	818	110	1828
Foot-Foot†	12	744	-168.88	79.11	1.78	0.07	33.07	18.23	0.43	0.85	917	223	1828
Transverse left arm-right leg†	8	693	-192.43	70.17	1.83	0.08	15.44	17.70	0.43	0.82	1008	430	2187
Transverse right arm-left leg†	8	685	-252.89	58.87	1.92	0.07	31.62	1266.00	0.65	0.87	928	260	1828
Whole Body†	7	826	-243.06	68.67	2.12	0.07	69.42	9.57	0.70	0.81	1160	523	2187

Table 3.4. Fixed effect coefficients from linear mixed effects model for fixed-distance BIA measurements using needle electrodes. Asterisks (*) indicate the measurement was on the downslope side of the body.

			Fixed effects										
Body Segment	Bodies	n	Intercept	Intercept S.E.	TBS^2	TBS^2 S.E.	BIA	BIA S.E.	Marginal R^2	Conditional R^2	ADD_{max} mean	ADD_{max} minimum	ADD_{max} maximum
Midfemur	27	451	-31.19	97.76	2.21	0.15	20.04	8.60	0.23	0.94	1551	47	5819
Midfemur*	25	433	-46.58	213.42	2.79	0.20	8.82	1.18	0.67	0.88	1668	47	6072
Midhumerus	22	276	-124.68	42.44	1.77	0.10	9.24	3.08	0.44	0.91	820	47	1976
Midhumerus*	23	392	33.81	200.83	2.15	0.14	17.03	6.01	0.13	0.95	1286	47	6128

This resource was prepared by the author(s) using Federal funds provided by the U.S. Department of Justice. Opinions or points of view expressed are those of the author(s) and do not necessarily reflect the official position or policies of the U.S. Department of Justice.

Table 3.5. Equations used to correct BIA resistance, reactance, and impedance readings to temperature using four different models. (c=corrected, m=measured, T=temperature, T20=20° C, R=resistance, X=reactance, Z=impedance).

Model	Equation
Random Intercept	$R_c = 1.7 \cdot 10^2 + 4.5 \cdot 10^{-10} \cdot BIA_m - 1.4 \cdot 10^{-9} \cdot (T_{20} - T_m)$ $X_c = 8.8 + 6.1 \cdot 10^{-14} \cdot BIA_m - 1.\ 8 \cdot 10^{-13} \cdot (T_{20} - T_m)$ $Z_c = (R_c^2 + X_c^2)^{0.5}$
Multiple Regression	$R_c = -25.87 + 1.32 \cdot BIA_m - 2.99 \cdot (T_{20} - T_m)$ $X_c = 3.63 + 0.61 \cdot BIA_m + 0.06 \cdot (T_{20} - T_m)$ $Z_c = (R_c^2 + X_c^2)^{0.5}$
2.5 Percent Correction	No correction reported for R_c No correction reported for X_c $Z_c = Z_m - \lvert T_{20} \cdot 0.025 \rvert$
Percent Correction	$R_c = R_m - \lvert T_{20} \cdot 0.014 \rvert$ $X_c = X_m - \lvert T_{20} \cdot 0.300 \rvert$ $Z_c = (R_c^2 + X_c^2)^{0.5}$

FIGURES

Fig- 1

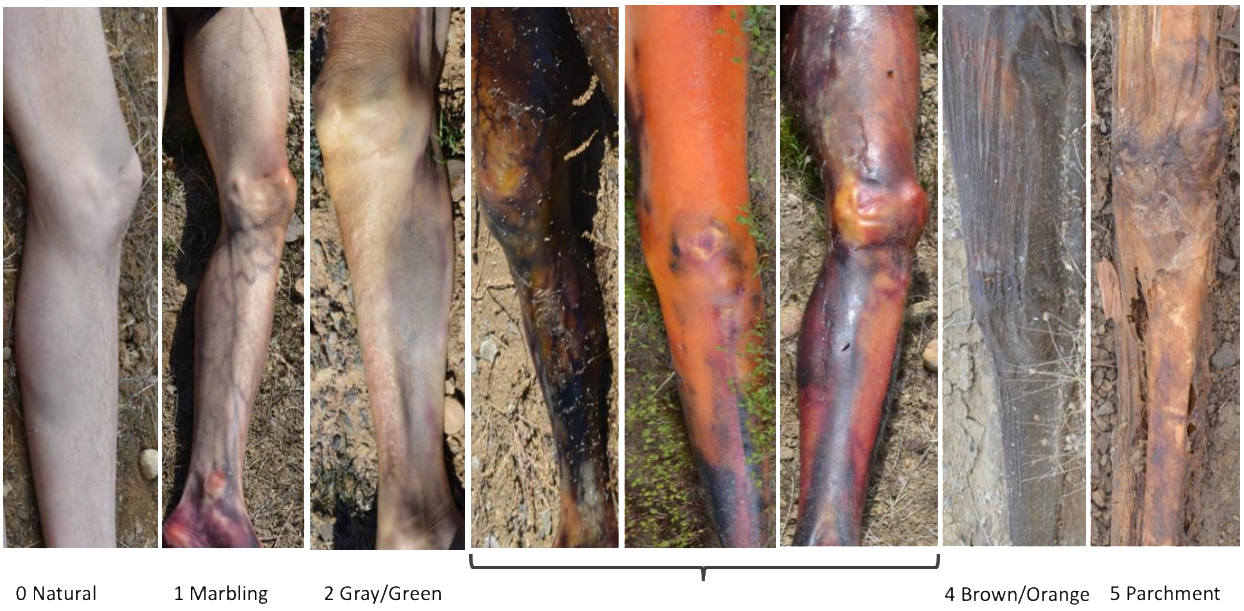

Figure 3.1. Changes in color seen throughout the decomposition process

Figure 3.2. Changes in moisture seen throughout the decomposition trajectory.

This resource was prepared by the author(s) using Federal funds provided by the U.S. Department of Justice. Opinions or points of view expressed are those of the author(s) and do not necessarily reflect the official position or policies of the U.S. Department of Justice.

Figure 3.3. Changes in tissue quality over the decomposition trajectory

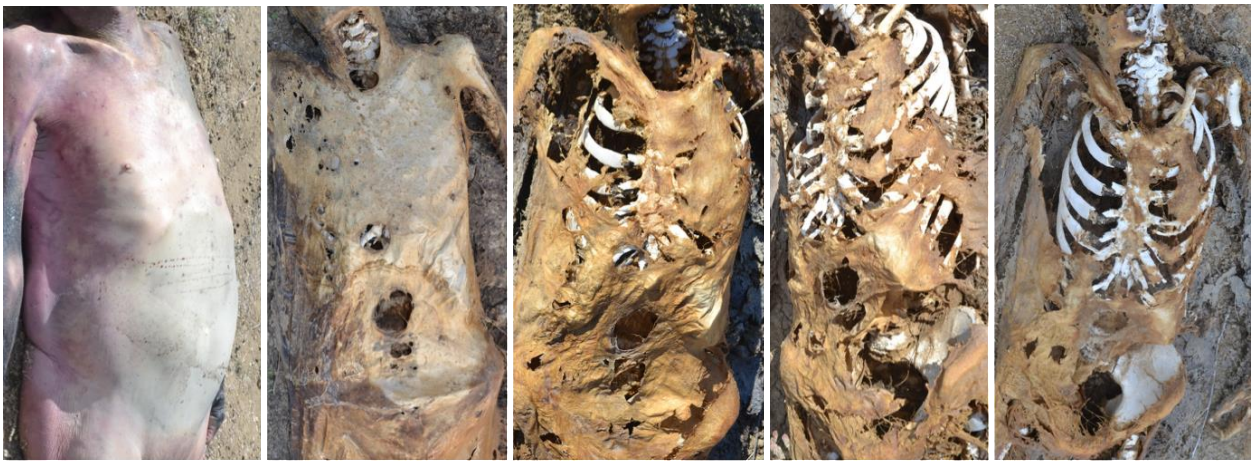

Figure 3.4. Changes in skeletonization seen in the thorax.

This resource was prepared by the author(s) using Federal funds provided by the U.S. Department of Justice. Opinions or points of view expressed are those of the author(s) and do not necessarily reflect the official position or policies of the U.S. Department of Justice.

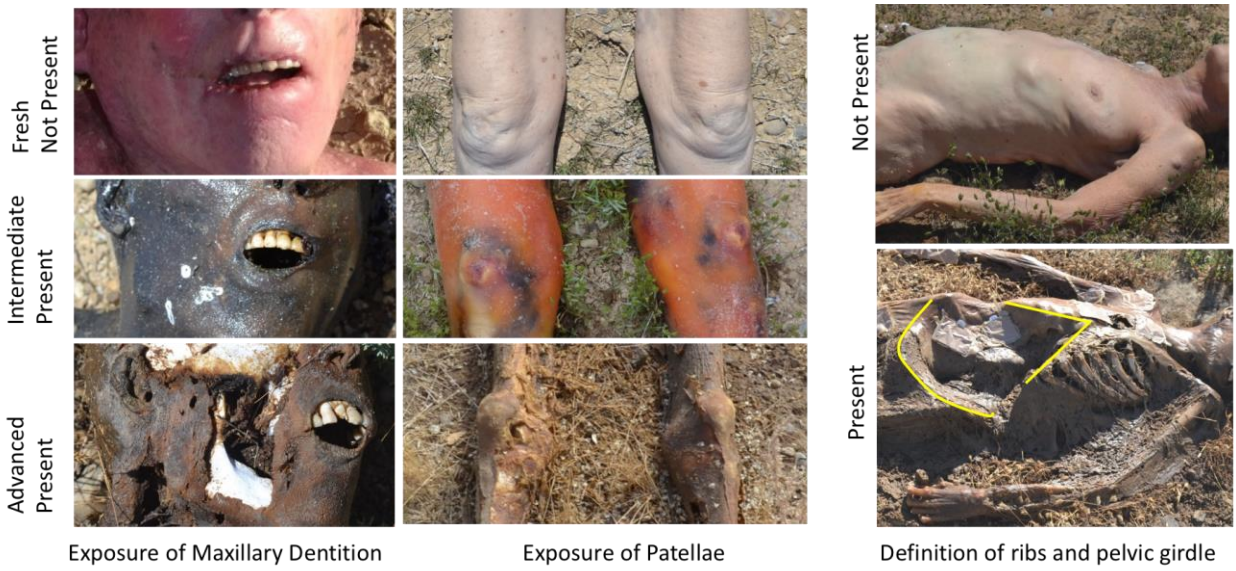

Figure 3.5. Qualitative filters used in the scoring of the total body desiccation score.

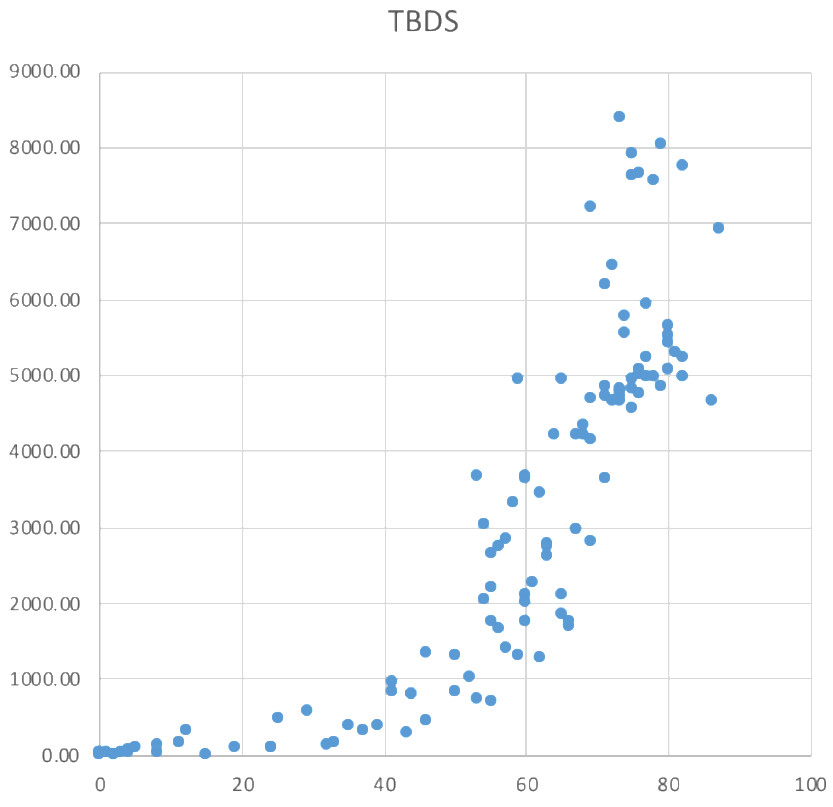

Figure 3.6. Accumulated degree days graphed with total body desiccation score.

This resource was prepared by the author(s) using Federal funds provided by the U.S. Department of Justice. Opinions or points of view expressed are those of the author(s) and do not necessarily reflect the official position or policies of the U.S. Department of Justice.

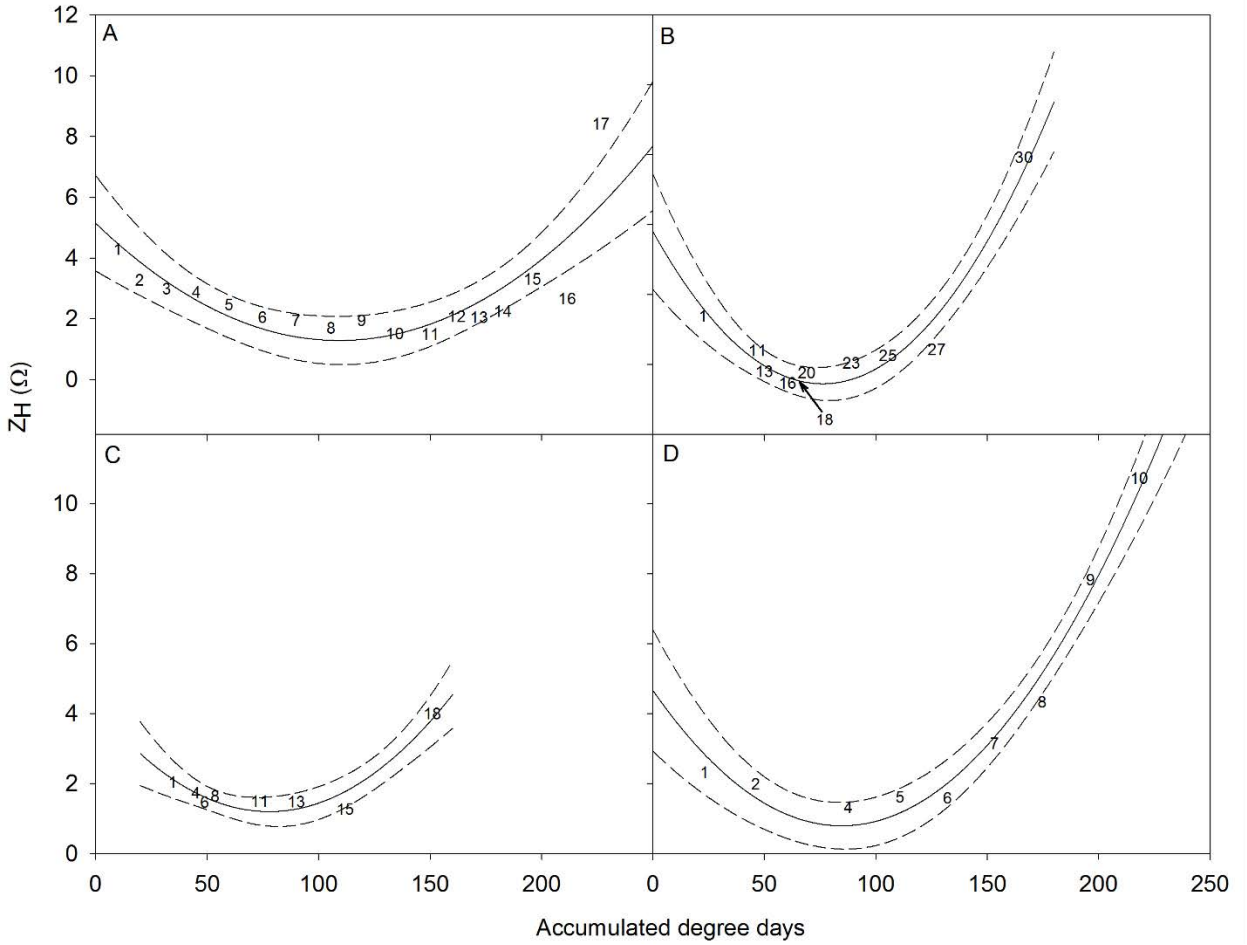

Figure 3.7. Relationship between Z_H and ADD for cadavers. The numeric value of the symbols represents the PMI in days. Quadratic regressions were used to fit solid lines. Dashed lines represent 95% confidence limits. (Hansen et al. 2017).

This resource was prepared by the author(s) using Federal funds provided by the U.S. Department of Justice. Opinions or points of view expressed are those of the author(s) and do not necessarily reflect the official position or policies of the U.S. Department of Justice.

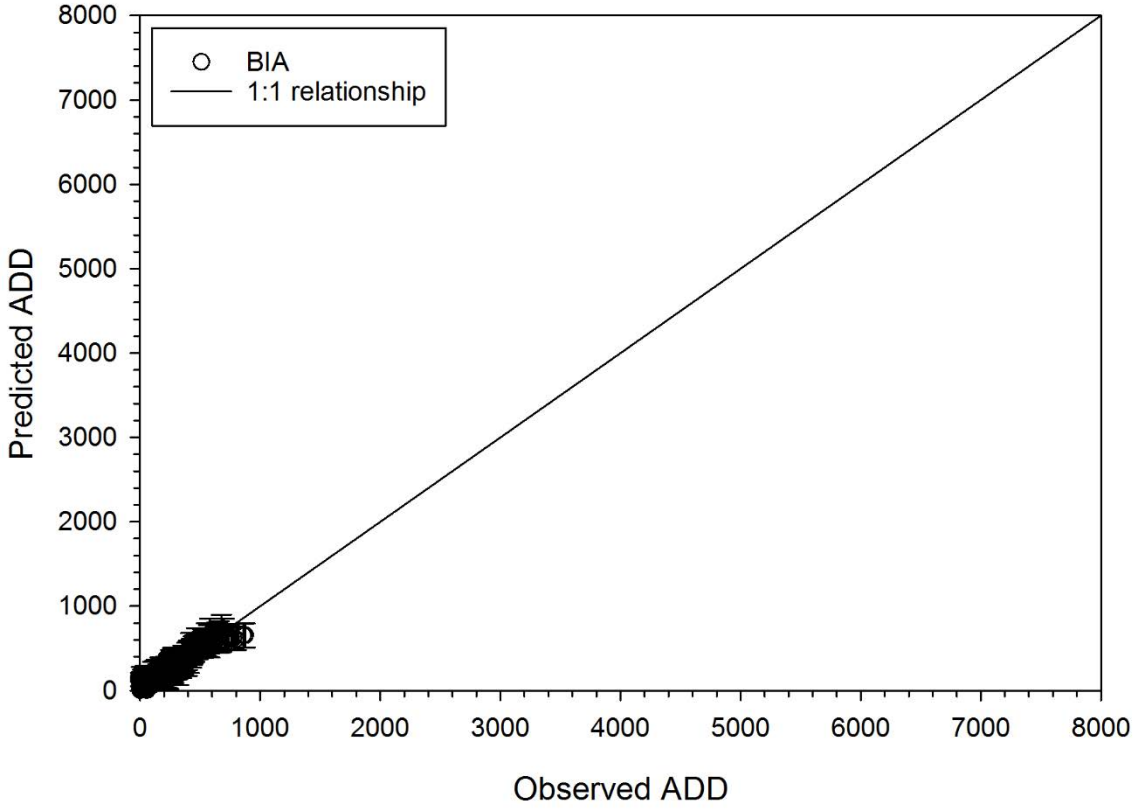

Figure 3.8. Observed versus predicted ADD for variable-distance BIA measured using needle electrodes and anatomical landmarks to isolate the hand-foot body segment on the upslope side of the donor. Error bars represent the 95% prediction interval. The line represents the 1:1 relationship between observed and predicted ADD.

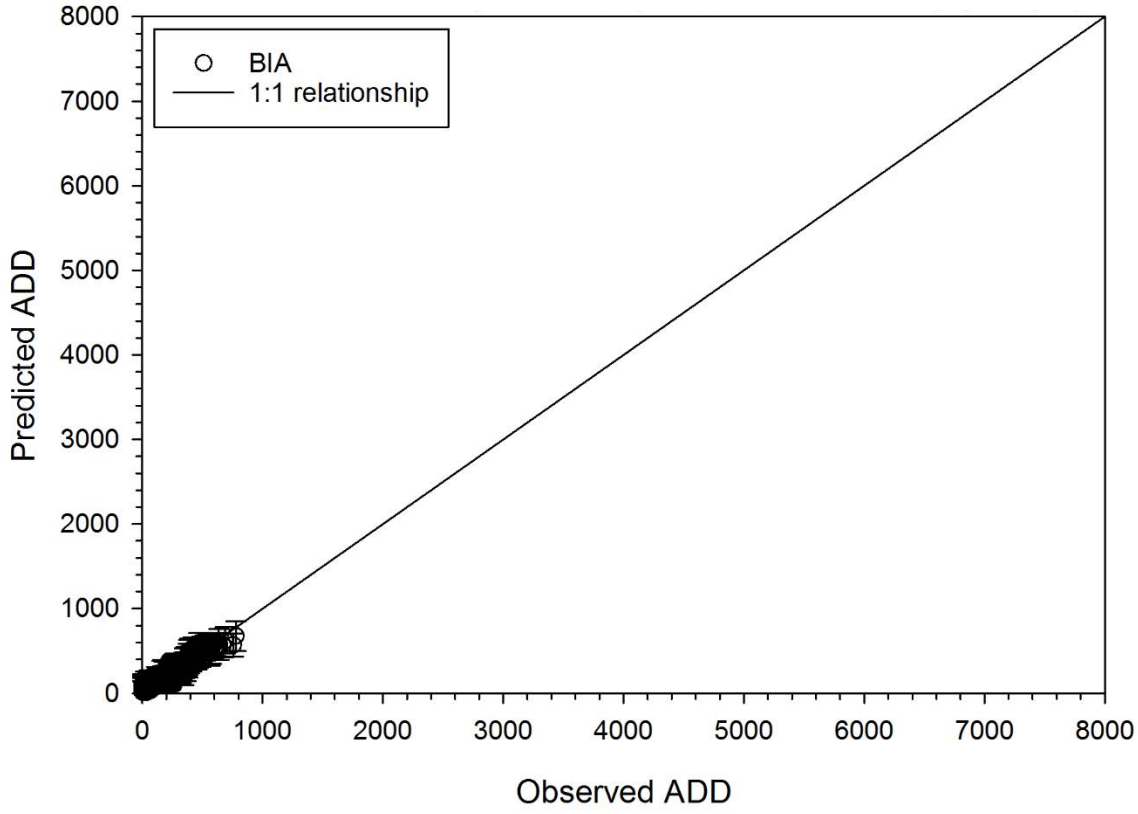

Figure 3.9. Observed versus predicted ADD for variable-distance BIA measured using needle electrodes and anatomical landmarks to isolate the hand-shoulder body segment on the upslope side of the donor. Error bars represent the 95% prediction interval. The line represents the 1:1 relationship between observed and predicted ADD.

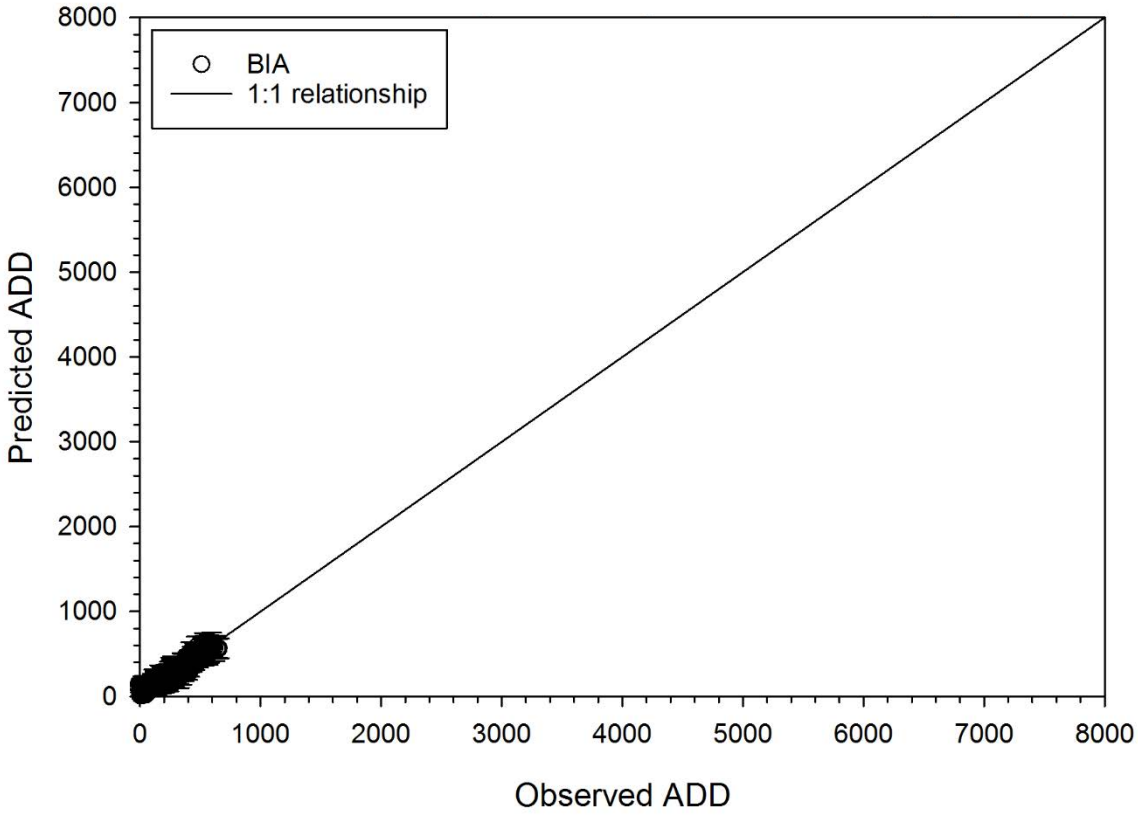

Figure 3.10. Observed versus predicted ADD for variable-distance BIA measured using needle electrodes and anatomical landmarks to isolate the shoulder-foot body segment on the upslope side of the donor. Error bars represent the 95% prediction interval. The line represents the 1:1 relationship between observed and predicted ADD.

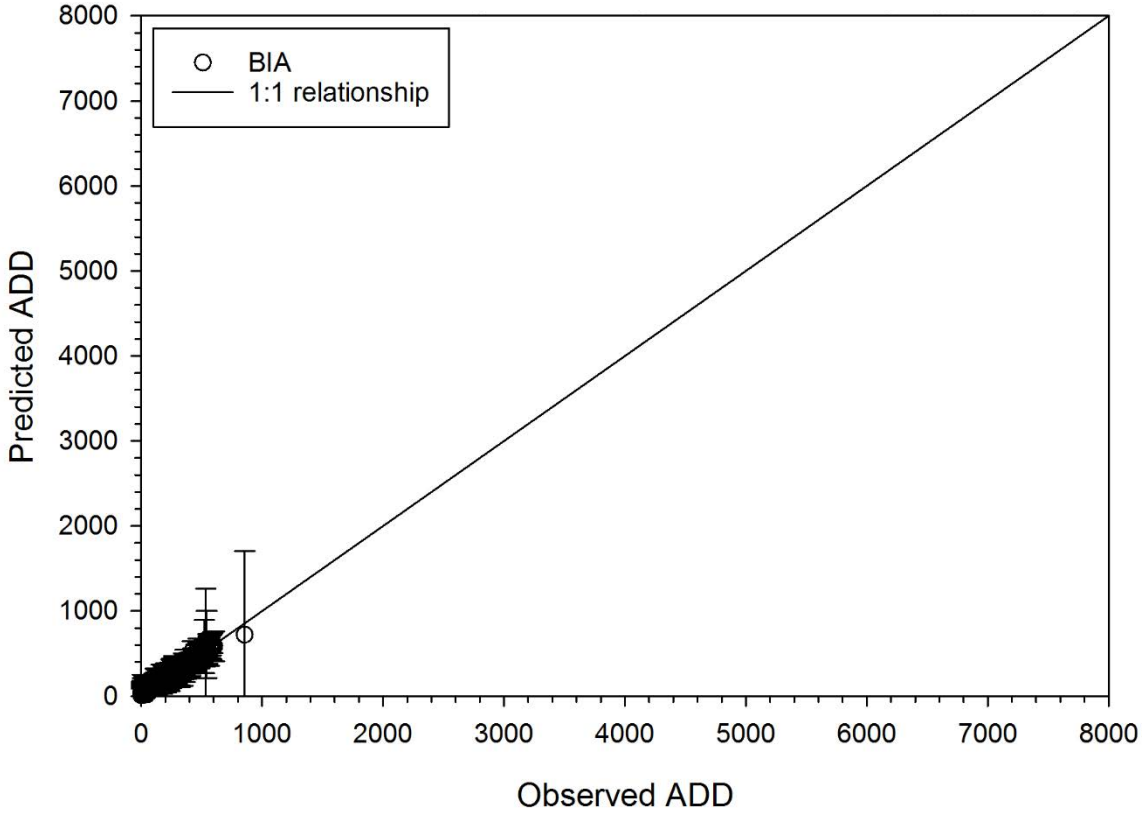

Figure 3.11. Observed versus predicted ADD for variable-distance BIA measured using needle electrodes and anatomical landmarks to isolate the shoulder-thigh body segment on the upslope side of the donor. Error bars represent the 95% prediction interval. The line represents the 1:1 relationship between observed and predicted ADD.

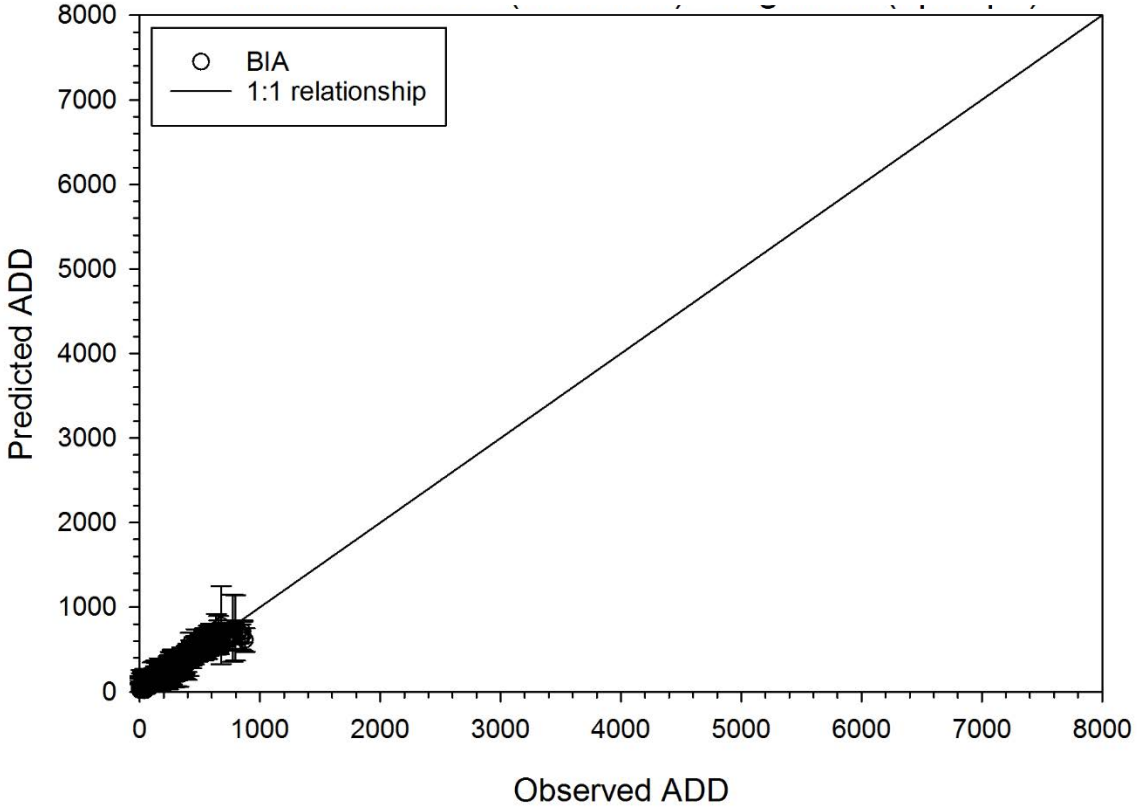

Figure 3.12. Observed versus predicted ADD for variable-distance BIA measured using needle electrodes and anatomical landmarks to isolate the thigh-foot body segment on the upslope side of the donor. Error bars represent the 95% prediction interval. The line represents the 1:1 relationship between observed and predicted ADD.

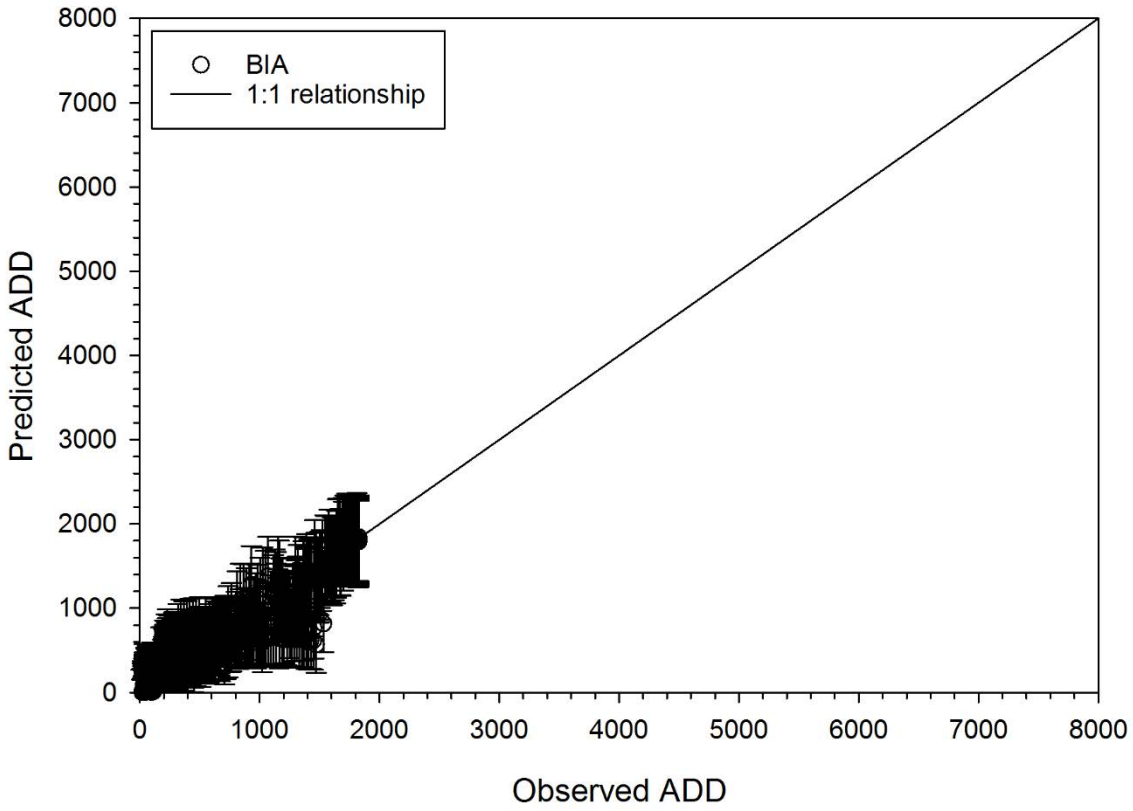

Figure 3.13. Observed versus predicted ADD for variable-distance BIA measured using needle electrodes positioned on the hands and feet to isolate the hand-foot body segment on the upslope side of the donor. Error bars represent the 95% prediction interval. The line represents the 1:1 relationship between observed and predicted ADD.

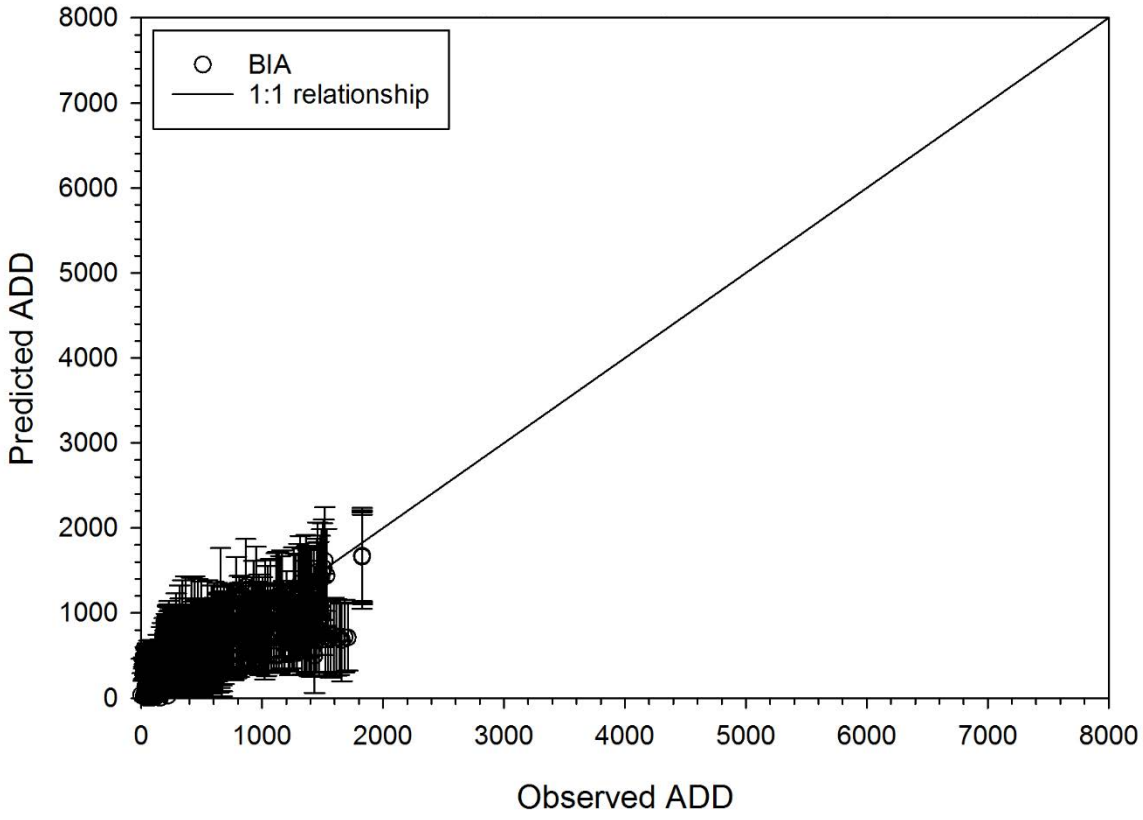

Figure 3.14. Observed versus predicted ADD for variable-distance BIA measured using needle electrodes positioned on the hands and feet to isolate the hand-foot body segment on the downslope side of the donor. Error bars represent the 95% prediction interval. The line represents the 1:1 relationship between observed and predicted ADD.

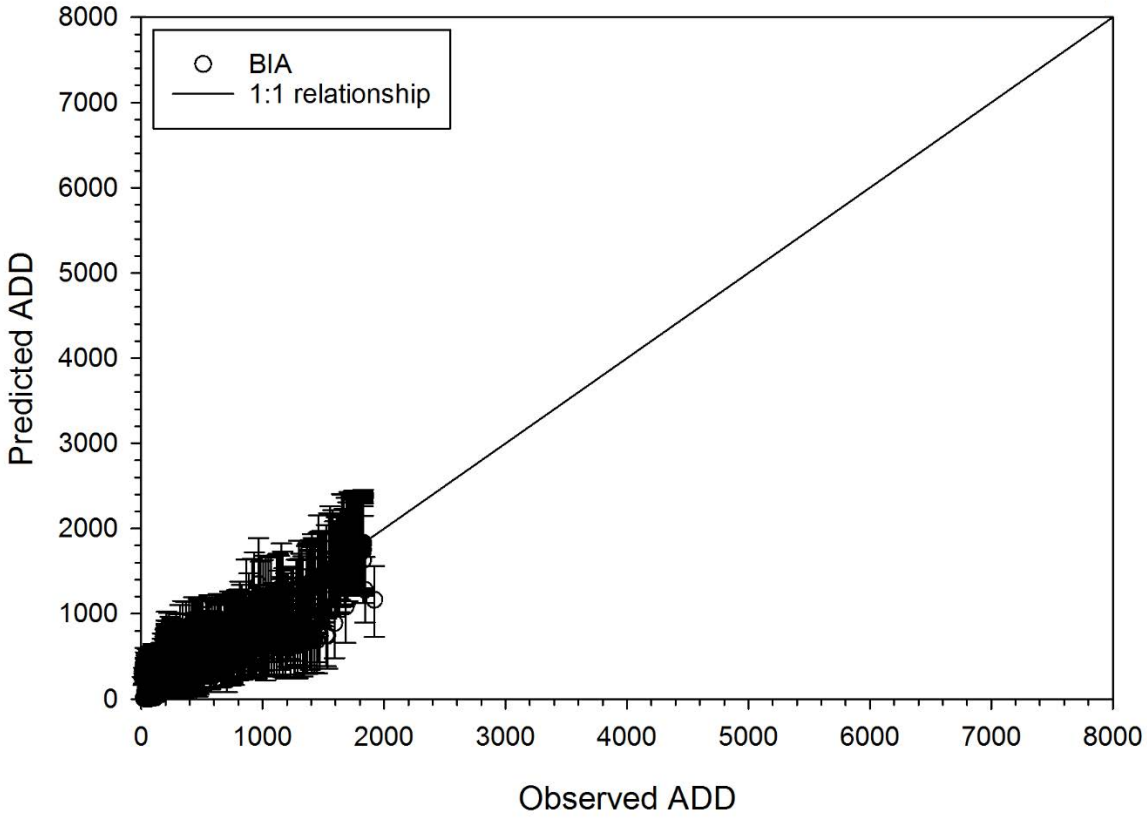

Figure 3.15. Observed versus predicted ADD for variable-distance BIA measured using needle electrodes positioned on the hands and feet to isolate the hand-shoulder body segment on the upslope side of the donor. Error bars represent the 95% prediction interval. The line represents the 1:1 relationship between observed and predicted ADD.

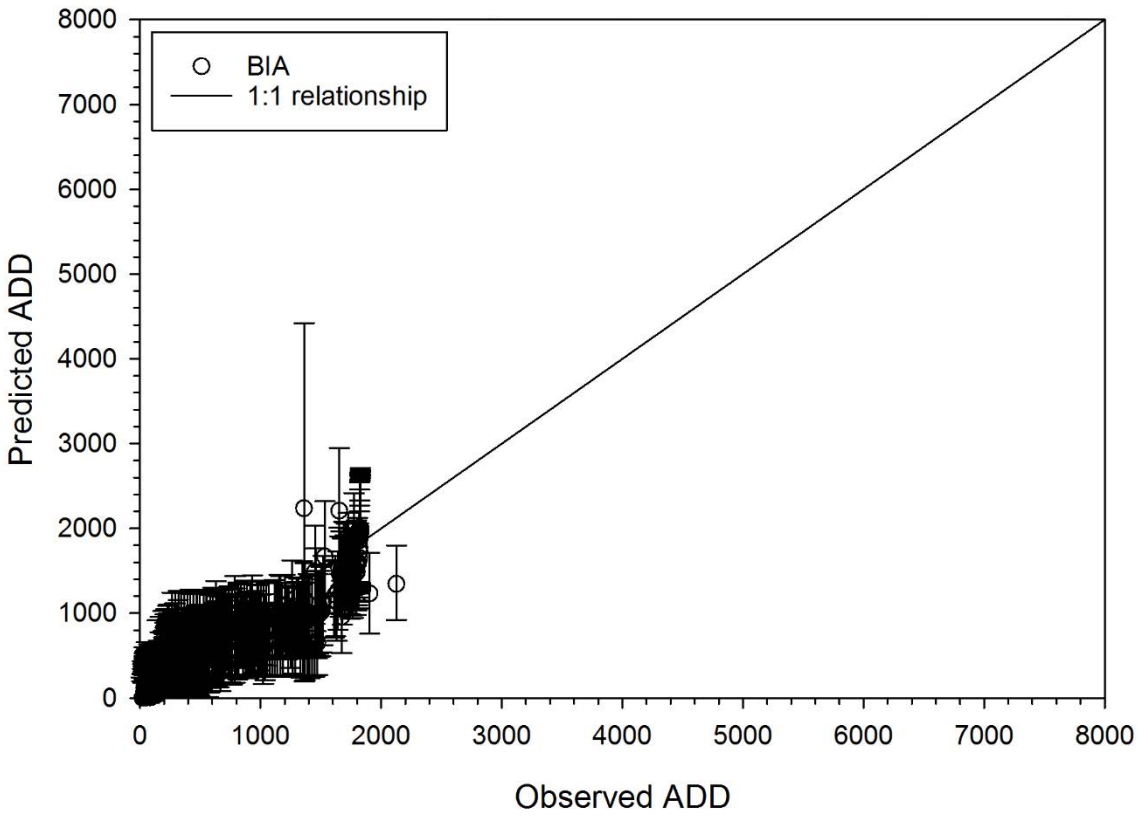

Figure 3.16. Observed versus predicted ADD for variable-distance BIA measured using needle electrodes positioned on the hands and feet to isolate the hand-shoulder body segment on the downslope side of the donor. Error bars represent the 95% prediction interval. The line represents the 1:1 relationship between observed and predicted ADD.

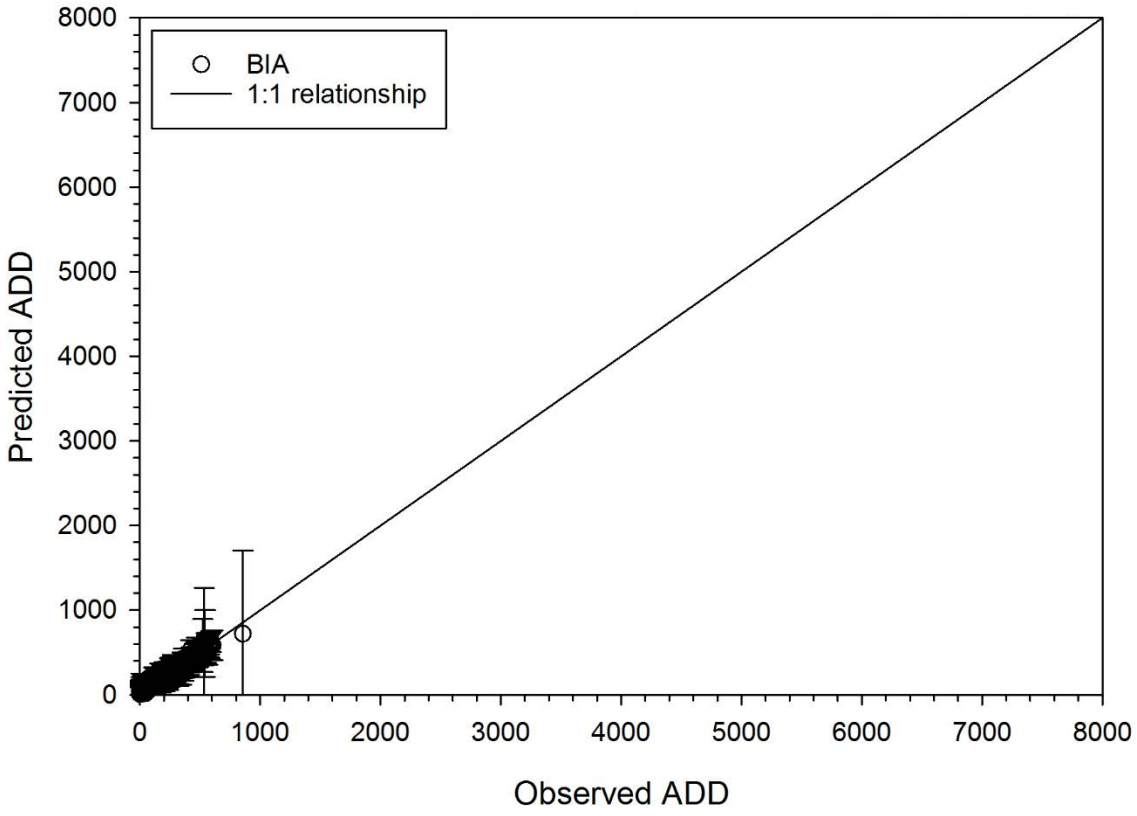

Figure 3.17. Observed versus predicted ADD for variable-distance BIA measured using needle electrodes positioned on the hands and feet to isolate the shoulder-thigh body segment on the upslope side of the donor. Error bars represent the 95% prediction interval. The line represents the 1:1 relationship between observed and predicted ADD.

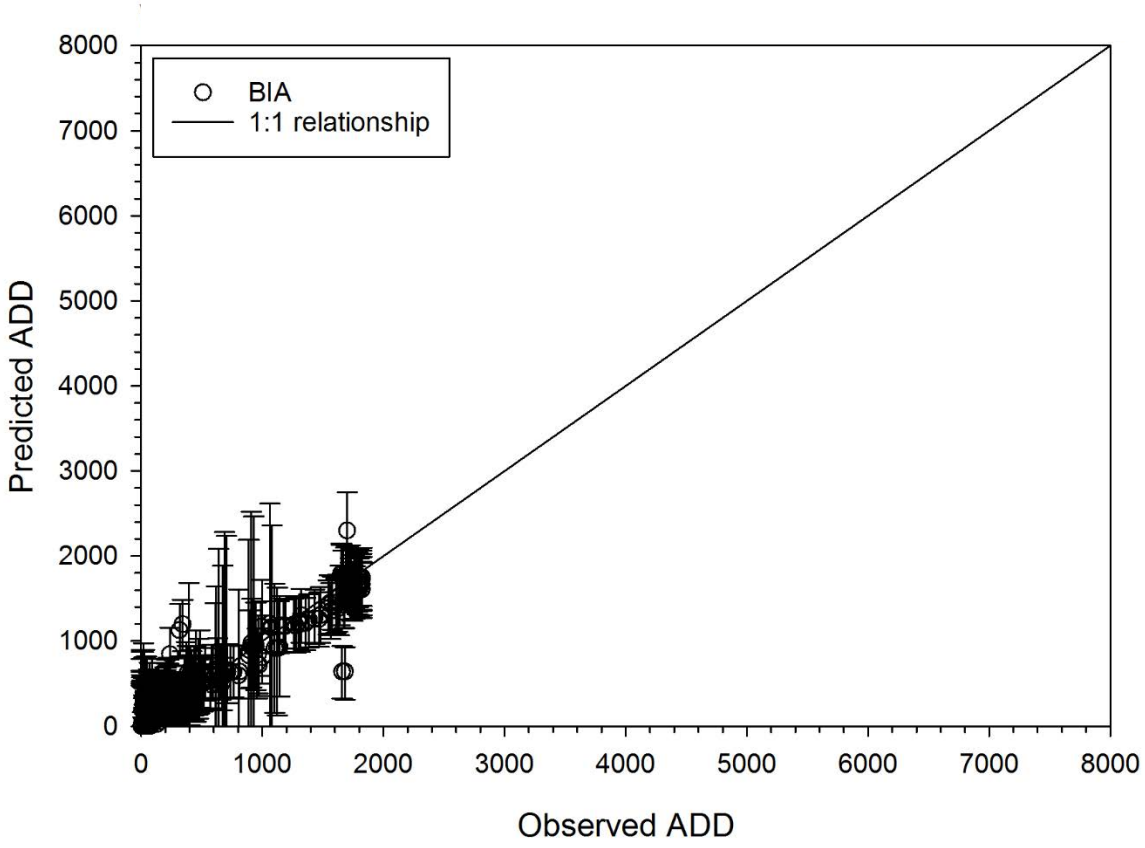

Figure 3.18. Observed versus predicted ADD for variable-distance BIA measured using needle electrodes positioned on the hands and feet to isolate the shoulder-thigh body segment on the downslope side of the donor. Error bars represent the 95% prediction interval. The line represents the 1:1 relationship between observed and predicted ADD.

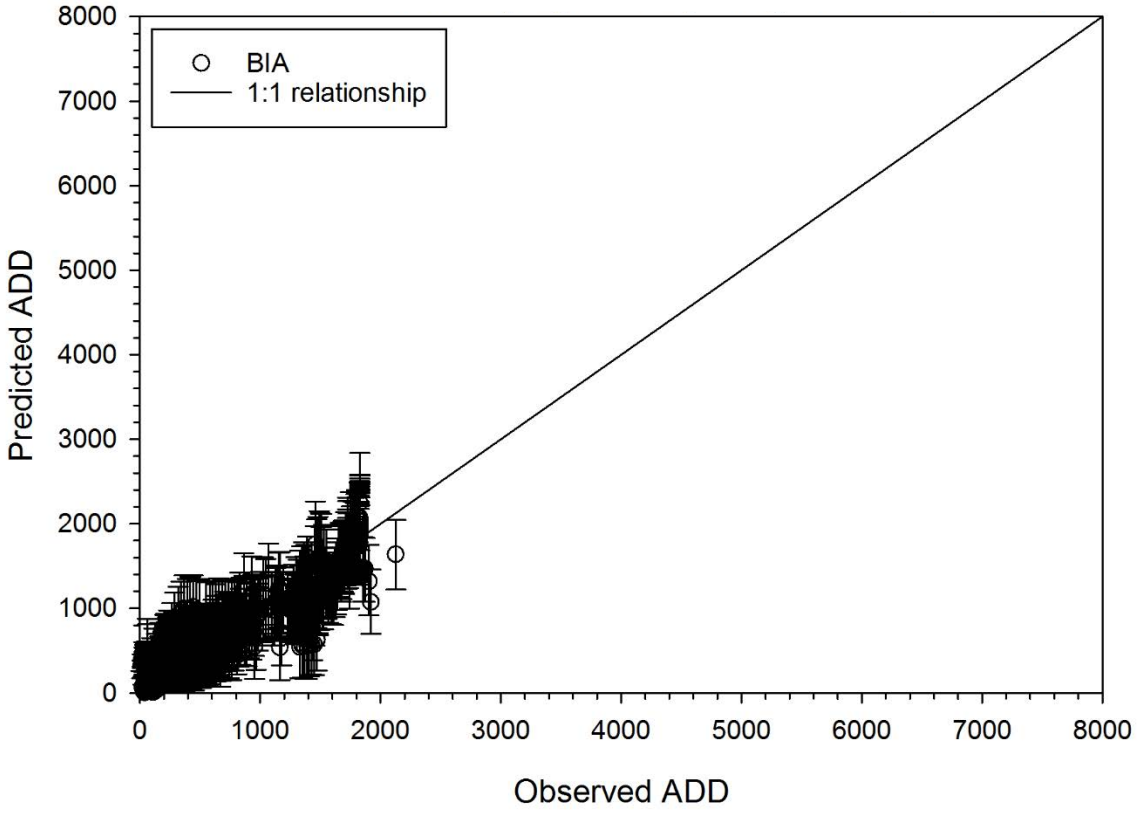

Figure 3.19. Observed versus predicted ADD for variable-distance BIA measured using needle electrodes positioned on the hands and feet to isolate the thigh-foot body segment on the upslope side of the donor. Error bars represent the 95% prediction interval. The line represents the 1:1 relationship between observed and predicted ADD.

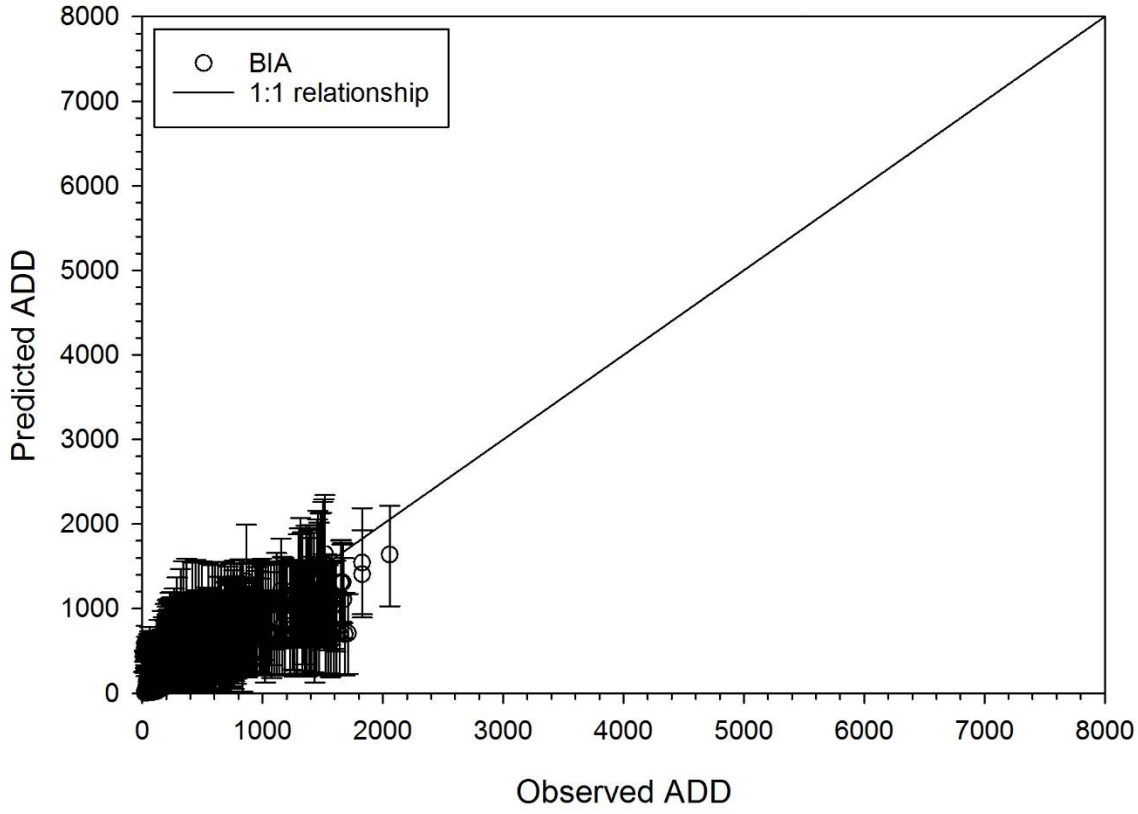

Figure 3.20. Observed versus predicted ADD for variable-distance BIA measured using needle electrodes positioned on the hands and feet to isolate the thigh-foot body segment on the downslope side of the donor. Error bars represent the 95% prediction interval. The line represents the 1:1 relationship between observed and predicted ADD.

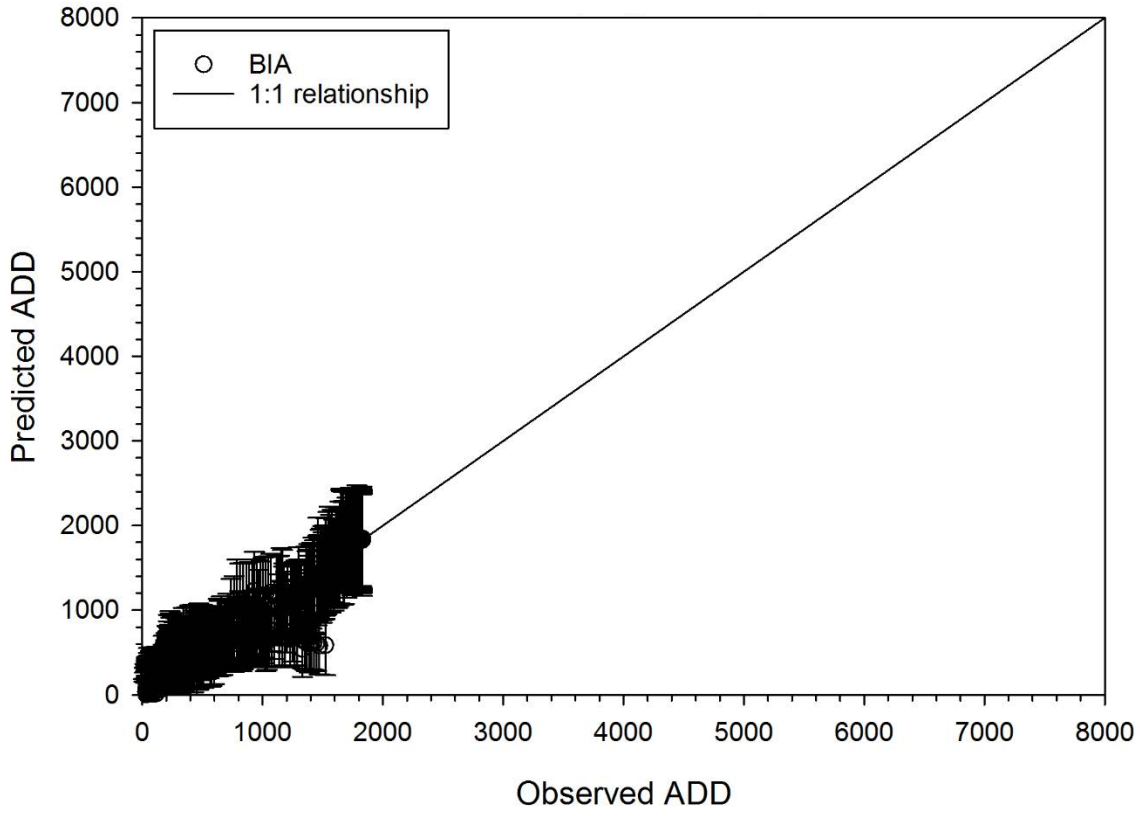

Figure 3.21. Observed versus predicted ADD for variable-distance BIA measured using needle electrodes positioned on the hands and feet to isolate the hand-hand body segment of the donor. Error bars represent the 95% prediction interval. The line represents the 1:1 relationship between observed and predicted ADD.

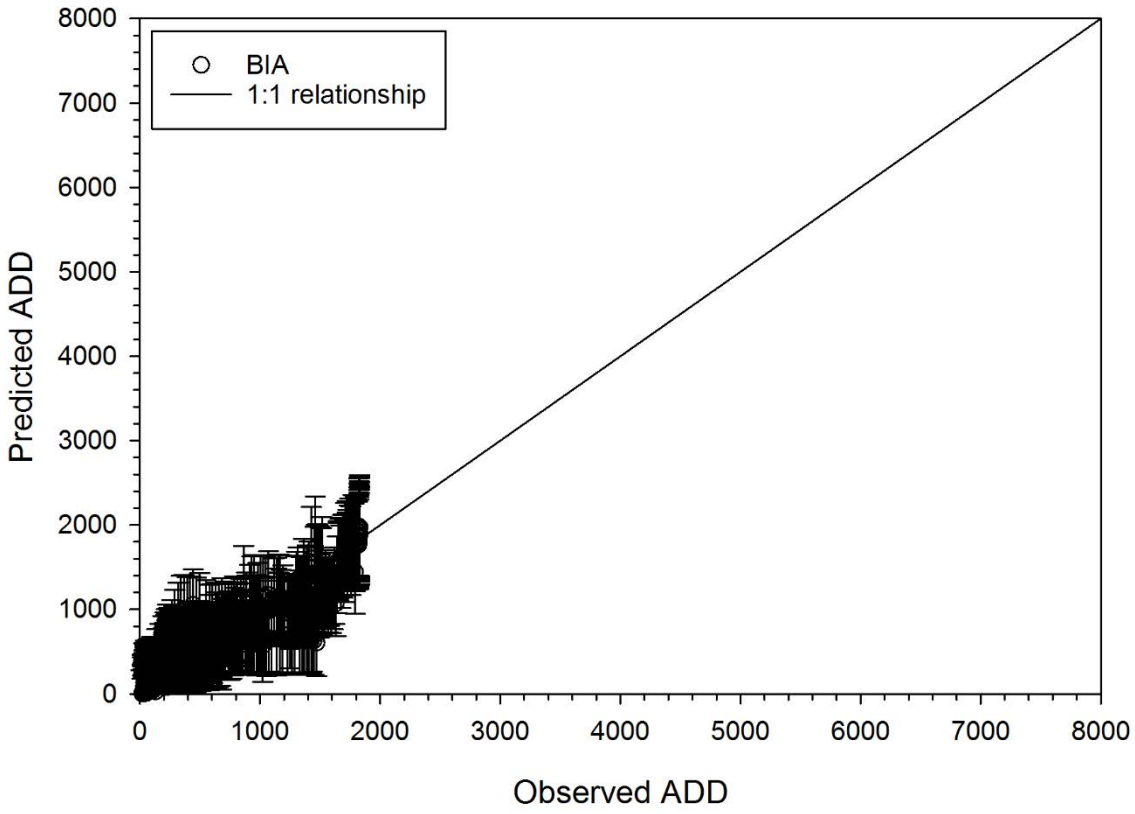

Figure 3.22. Observed versus predicted ADD for variable-distance BIA measured using needle electrodes positioned on the hands and feet to isolate the foot-foot body segment of the donor. Error bars represent the 95% prediction interval. The line represents the 1:1 relationship between observed and predicted ADD.

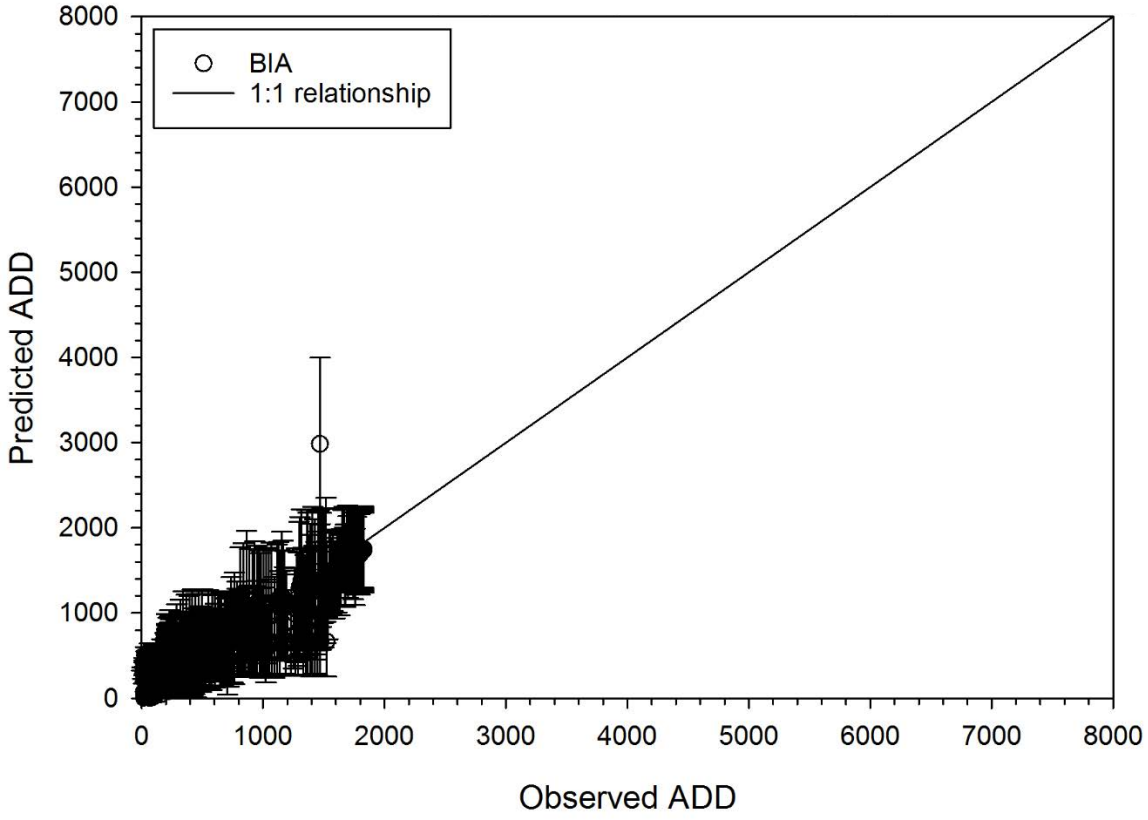

Figure 3.23. Observed versus predicted ADD for variable-distance BIA measured using needle electrodes positioned on the hands and feet to isolate the transverse (right arm – left leg) body segment of the donor. Error bars represent the 95% prediction interval. The line represents the 1:1 relationship between observed and predicted ADD.

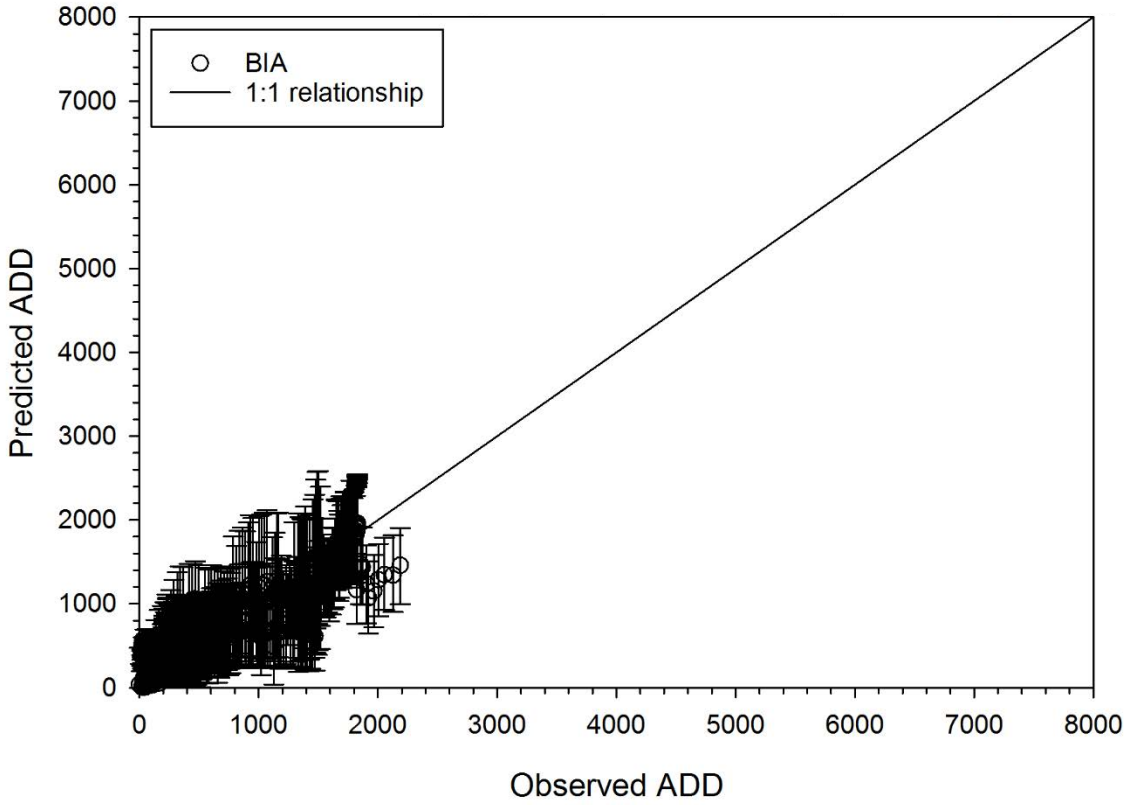

Figure 3.24. Observed versus predicted ADD for variable-distance BIA measured using needle electrodes positioned on the hands and feet to isolate the transverse (left arm – right leg) body segment of the donor. Error bars represent the 95% prediction interval. The line represents the 1:1 relationship between observed and predicted ADD.

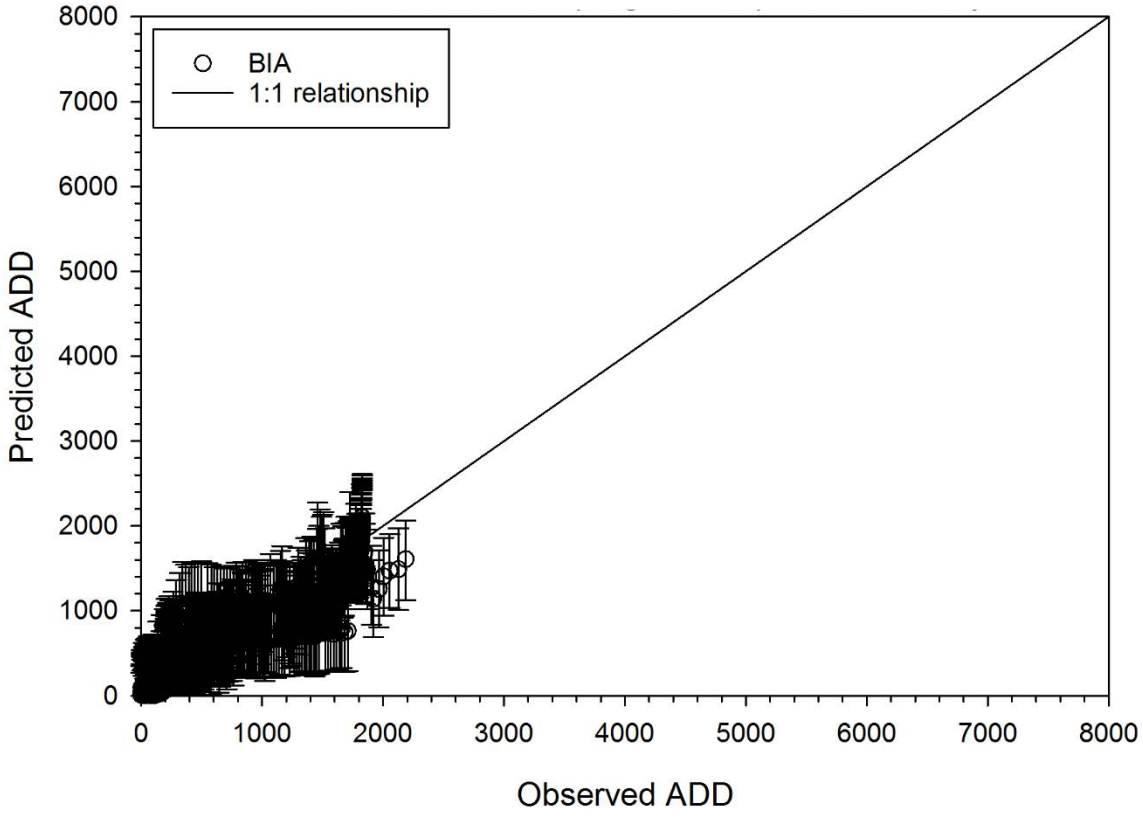

Figure 3.25. Observed versus predicted ADD for variable-distance BIA measured using needle electrodes positioned on the hands and feet to isolate the "whole body" body segment of the donor. Error bars represent the 95% prediction interval. The line represents the 1:1 relationship between observed and predicted ADD.

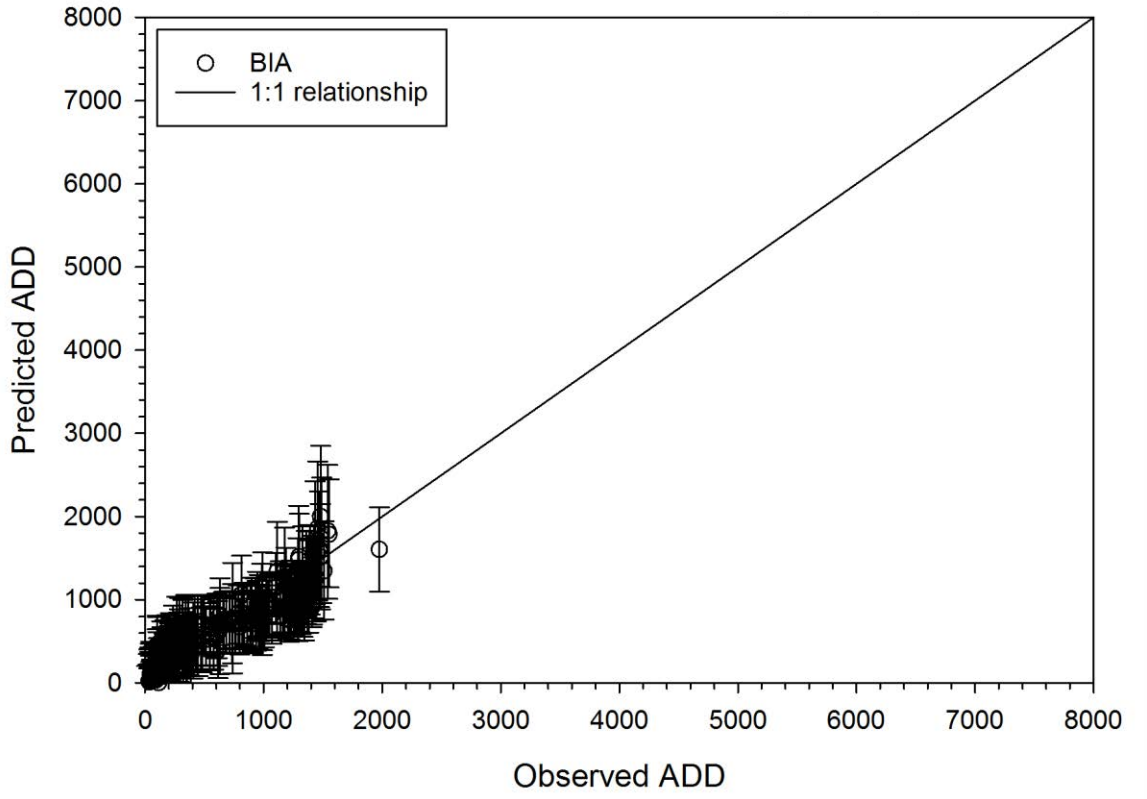

Figure 3.26. Observed versus predicted ADD for fixed-distance BIA measurements using needle electrodes positioned at the mid-humerus on the upslope side of the donor. Error bars represent the 95% prediction interval. The line represents the 1:1 relationship between observed and predicted ADD.

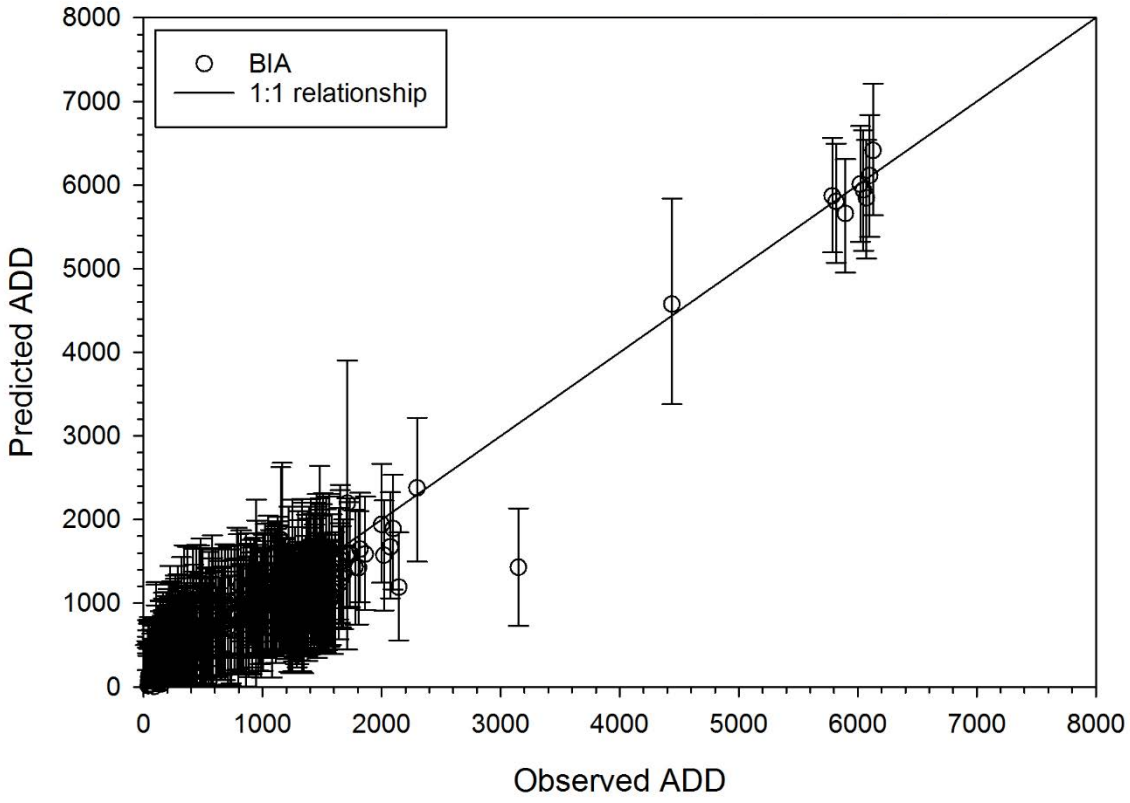

Figure 3.27. Observed versus predicted ADD for fixed-distance BIA measurements using needle electrodes positioned at mid-humerus on the downslope side of the donor. Error bars represent the 95% prediction interval. The line represents the 1:1 relationship between observed and predicted ADD.

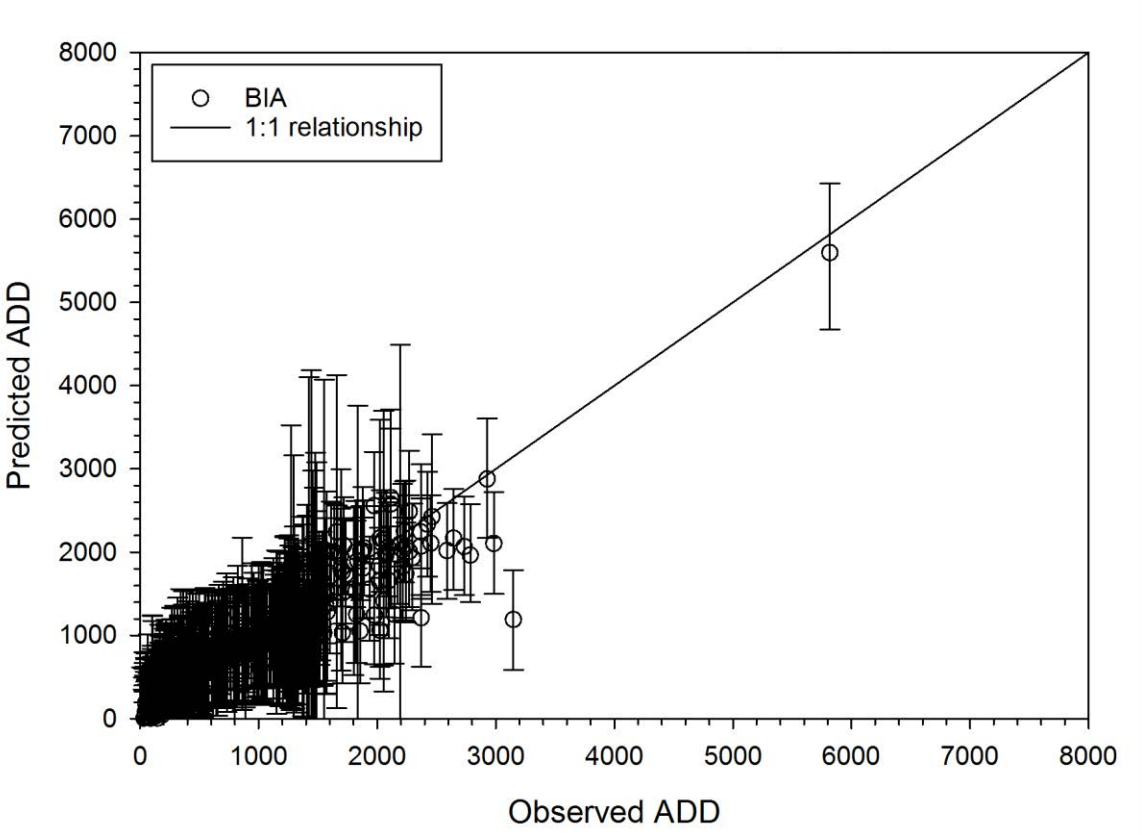

Figure 3.29. Observed versus predicted ADD for fixed-distance BIA measurements using needle electrodes positioned at mid-femur on the upslope side of the donor. Error bars represent the 95% prediction interval. The line represents the 1:1 relationship between observed and predicted ADD.

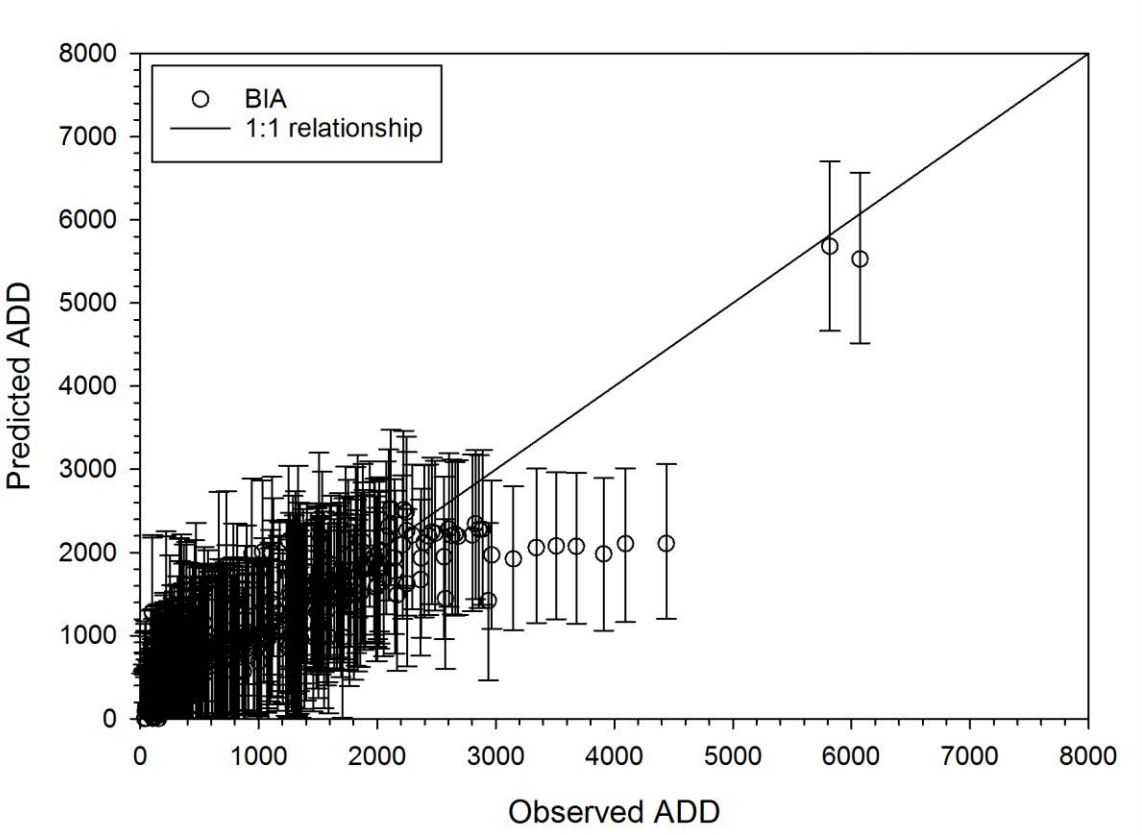

Figure 3.30. Observed versus predicted ADD for fixed-distance BIA measurements using needle electrodes positioned at mid-femur on the downslope side of the donor. Error bars represent the 95% prediction interval. The line represents the 1:1 relationship between observed and predicted ADD.

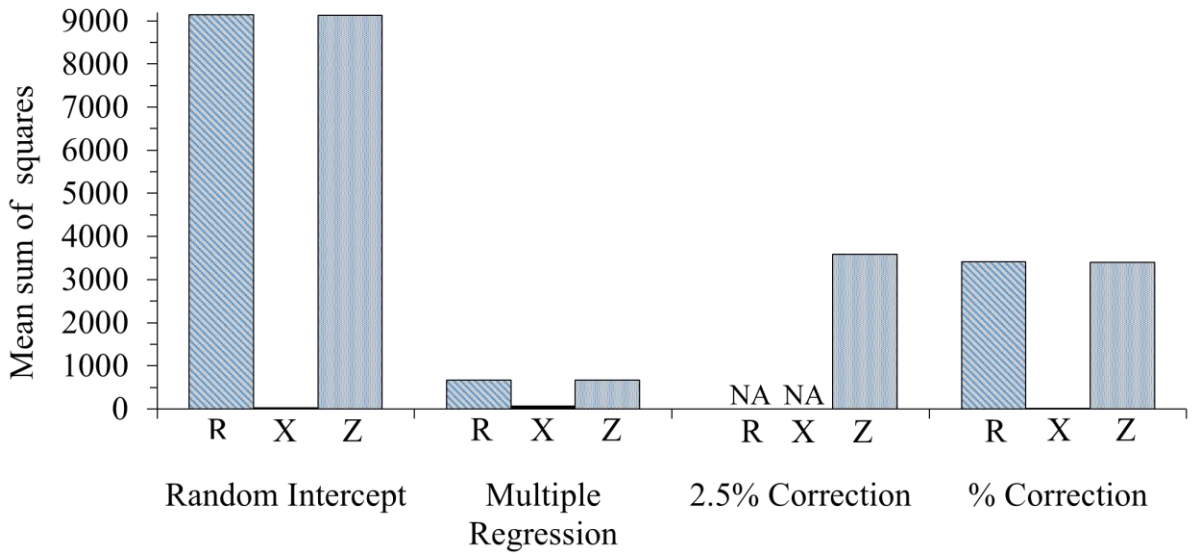

Figure 3.31. Mean sum of squares for the four temperature correction methods and BIA metrics R, X, and Z.

Appendix 1. Publications

List of Publications and Presentations that incorporated this grant

Connor, M., C. Baigent, and E. S. Hansen. *In review*. Measuring desiccation using qualitative changes: a step toward determining regional decomposition sequences. Journal of Forensic Sciences.

Connor, M., C Baigent, E. S. Hansen. (2017). Measuring Desiccation using Morphological Changes: The Total Body Desiccation Score. Proceedings of the American Academy of Forensic Sciences 69th Annual Meeting, New Orleans.

Connor, M., E. S. Hansen, C Baigent. (2017). Measuring desiccation: A system using bioelectrical impedance analysis. NIJ Symposium. Proceedings of the American Academy of Forensic Sciences 69th Annual Meeting, New Orleans.

Connor, M, C. Baigent, E. S. Hansen (2018). Deconstructing Desiccation and Decomposition. Proceedings of the American Academy of Forensic Sciences 70th Annual Meeting, Seattle, Washington.

Connor, M., C. Baigent, E. S. Hansen (2017). Testing the Use of Pigs as Human Proxies in Decomposition Studies. Journal of Forensic Sciences, available online doi: 10.1111/1556-4029.13727.

Hansen, E, S. Reck, M. Connor (2017). Correlation of Bioelectric Impedance Metrics to Accumulated Degree Days for Among Body Segments using Gel Pad Electrodes. Proceedings of the American Academy of Forensic Sciences 69th Annual Meeting, New Orleans.

Hansen, E. S., M Connor, C Baigent. (2017). Bioelectrical Impedance Analysis as a Technique for Estimating the Post-Mortem Interval in Human Remains. Proceedings of the American Academy of Forensic Sciences 69th Annual Meeting, New Orleans.

Hansen, E. S., C. Baigent, M. Connor (2018). A Comparison of Bioelectrical Impedance Analysis Techniques for Estimating Postmortem Interval (PMI). Proceedings of the American Academy of Forensic Sciences 70th Annual Meeting, Seattle, Washington.

Hansen, E. S., C. Baigent, S. Reck, and M. Connor. (2018). Bioelectrical Impedance as a Technique for Estimating Postmortem Interval. Journal of Forensic Sciences 63(4):1186-1190.

Reck, S. I., E. S. Hansen, and M. A. Connor (2017). Correlation of bioelectric impedance metrics to accumulated degree days among body segments using gel pad electrodes (Poster). Student Showcase, Colorado Mesa University, Grand Junction, CO.

JOURNAL OF FORENSIC SCIENCES

J Forensic Sci, July 2018, Vol. 63, No. 4
doi: 10.1111/1556-4029.13695
Available online at: onlinelibrary.wiley.com

PAPER

PATHOLOGY/BIOLOGY

Eriek S. Hansen,[1] Ph.D.; Christiane Baigent,[2] M.Sc.; Sophia I. Reck,[1] B.S.; and Melissa Connor,[2] Ph.D.

Bioelectrical Impedance as a Technique for Estimating Postmortem Interval*,†,‡

ABSTRACT: Estimation of postmortem interval (PMI) is a critical component of death investigation. A cadaver can be hypothesized to be a resistor–capacitor (RC) circuit the impedance (*Z*) of which changes in a quantifiable manner as the cadaver decomposes. This hypothesis was tested using bioelectrical impedance analysis (BIA) equipment to apply a current with a fixed amplitude at a single frequency to four cadavers over time and measuring two components of *Z*, resistance (*R*) and reactance (X_c). Quadratic regression analysis between *Z* and accumulated degree days (ADD) showed a statistically significant parabolic relationship. The parabolic relationship poses an initial challenge to the use of the method, and additional research is needed to address this issue. However, the results of the reported research support the hypothesis that *Z* measured using BIA has a relationship to PMI.

KEYWORDS: forensic science, forensic taphonomy, forensic pathology, forensic anthropology, postmortem interval, human decomposition, bioelectrical impedance analysis

The estimation of postmortem interval (PMI) is a critical component of medicolegal death investigation. Accurate PMI estimates have the potential to aid in identification of unknown remains, inform cause and manner of death, distinguish ante- and/or perimortem trauma and pathology from postmortem artifact, and facilitate suspect pool structure. While a critical investigative tool, PMI estimation is complex and becomes increasingly so as the PMI lengthens. Decomposition is a dynamic, but ultimately reductive, process. The rate and manner of reduction are dictated by extant biotic and abiotic variables within both the postdeposition environment and individual remains. Medicolegal professionals concerned with the estimation of PMI are limited by these dynamic, degenerative chronobiological changes; as PMI increases, the accuracy of methods for estimation decreases with a concomitant increase in error. Methods for early PMI estimation typically rely on physiochemical changes, which are diverse and variably applied. Examples include gross opacity of the sclera (1), vitreous chemistry (sodium, potassium, and chloride composition) (2), cadaver temperature collected from anatomically defined sites, including: neural (3), rectal (4), otic (5), and optic (6), spectrophotometric analysis of lividity (7), development and recession of rigor mortis (8), cellular content of cerebrospinal fluid (9), and postmortem changes to lactate and malate dehydrogenase concentration in the human liver (10). Late-stage estimation has traditionally been limited to macroscopic analysis of gross tissue change, including putrefaction, adipocere formation, and mummification (11). However, rate and trajectory of gross tissue change are dependent on variables within the postdeposition environment, including temperature, pH, partial pressure of atmospheric gasses, and insect, microbial, and faunal succession (12), making macroscopic methods both subjective and imprecise. In an effort to account for this broad suite of variables, Vass et al. (13) applied accumulated degree days (ADD) to the estimation of PMI. Megyesi et al. (14) expanded upon this model by defining a series of value-assigned categories of change to body regions, the sum of which yields a total body score (TBS). When applied to the model's given regression equation, TBS provides an estimate of ADD, which in turn produces an estimation of PMI when retrospectively applied to local temperature data. However, because a suite of variables beyond ambient temperature may affect the trajectory of decomposition, "universal" models governed by a single variable are inherently problematic. For example, the location of the temperature measurement can be a source of error (15,16). As a result, methods developed for predicting PMI have trended toward measuring changes in additional variables such as the temporal progression and succession of the necrobiome (17), and soil biogeochemical assessment (18). These methods attempt to measure and quantify the rate of change expressed by a biological phenomenon based on changes to composition attendant to the decomposition event and have potential for application for late-stage PMI estimation. In the pursuit of improving PMI estimates, bioelectrical impedance analysis (BIA) is presented as an alternative method.

Bioelectrical impedance analysis technology was developed for healthcare application, primarily for the estimation of

[1]Department of Biological Sciences, Colorado Mesa University, 1100 North Avenue, Grand Junction, CO 81501.
[2]Department of Social and Behavioral Sciences, Forensic Investigation Research Station, Colorado Mesa University, 1100 North Avenue, Grand Junction, CO 81501.

*Supported by Award No. 2015-DN-BX-K015, awarded by the National Institute of Justice, Office of Justice Programs, U.S. Department of Justice.

†The opinions, findings, and conclusions or recommendations expressed in this publication are those of the authors and do not necessarily reflect those of the Department of Justice.

‡Presented in part at the 69th Annual Scientific Meeting of the American Academy of Forensic Sciences, February 13-18, 2017, in New Orleans, LA.

Received 21 July 2017; and in revised form 08 Sep. 2017; 10 Oct. 2017; 24 Oct. 2017; accepted 25 Oct. 2017.

proximate body composition (water, lipid, and lipid-free dry masses) (19,20). In its constituent parts, the human body is composed of lipid-free mass (everything structural that is not body lipids, including visceral protein and bone mineral), total body water (composed of extracellular and intracellular fluids), and lipid mass. These structures possess variable impedance (Z) based on composition (e.g., electrolyte gradients in intra- and extracellular fluids have low Z, while lipids lack appreciable water content and are therefore poor conductors with high Z).

The Z of biological tissue is determined at the cellular and molecular level. The primary mechanisms include ionic conduction of proteins and other organic macromolecules, ionic diffusion processes at the site of the cellular membrane, and changes to cell membrane structure (21). Conceptually, the sum of these components comprises a resistor-capacitor (RC) circuit. Single-frequency BIA equipment functions by introducing a fixed alternating current between two electrodes attached to the cadaver, while concurrently measuring the voltage drop and phase lag within the same body segment using a second pair of electrodes attached to the cadaver. The BIA equipment records the measurements of the two components of Z: resistance (R) and capacitive reactance (X_c). R measurements can be conceptually understood as the opposition to electron flow through intracellular and extracellular electrolyte gradients when direct currents are used; measurements may therefore vary within and among tissues due to the structure, composition, and volume of intra- and extracellular fluids, whereas X_c is a measurement of capacitive reactance afforded by the phospholipid bilayer of cell membranes, the polarity of which results in the ability to hold a charge when alternating currents are used.

Single-frequency BIA generally uses a 50 kHz frequency and an alternating current with a fixed amplitude that is not measuring total body water but rather the weighted sum of extracellular and intracellular fluid resistivities (20). At 50 kHz, the penetration of the cell membrane is minimal (~25%), permitting estimation of the body's lipid-free mass and total body water but does not assess differences between extracellular fluid and intracellular fluid R (20). In addition, using a 50 kHz frequency maximizes X_c of skeletal muscle tissue (i.e., 50 kHz is the mean characteristic frequency of Cole-Cole models) (22).

The potential for forensic application of BIA is based on the dielectric properties of biological tissue. Changes to human cadavers during decomposition can be viewed as changes to the configuration of the RC circuit. Bioelectrical impedance quantifies changes to the circuit, which may be correlated with ADD, creating a powerful potential tool to estimate PMI. Decomposition includes many dynamic processes occurring simultaneously. However, viewing processes independently in the context of R and X_c facilitates an understanding of how the configuration of the RC circuit changes. Some of these relationships are inferred from the principles governing electricity and the well-understood physiochemical changes associated with decomposition. For example, as autolytic cellular destruction releases intracellular fluid into the extracellular fluid, a decrease in R is expected to follow. R is also expected to decrease with a decrease in extracellular ion concentration. Conversely, X_c and the number of intact cells have a positive relationship. Cell membranes act as capacitors (i.e., temporarily hold an electrical charge); postmortem cell autolysis decreases the volume of intact cell membranes resulting in a decrease in X_c. These patterns should correlate with the PMI.

Previous research demonstrated predictable postmortem changes in Z in nonhuman proxies. Querido (23,24) repeatedly observed an inverse relationship between Z and PMI using rats. A decrease in abdominal R attendant to increased PMI was also observed (25). Based on the dielectric properties of biological tissue and previous research in nonhuman vertebrates, this study hypothesized that decomposition changes the configuration of the human cadaver's RC circuit in quantifiable ways, which enables estimation of PMI. BIA is a method for measuring those changes in the RC circuit. The specific objective of this experiment was to evaluate the relationship between BIA metrics and PMI using the RC circuit between the hand and the foot. The objective of this research was not to develop predictive equations, but simply to establish that there is a relationship between Z and ADD. Additional research will be necessary to develop predictive equations.

Materials and Methods

Research Facility

Colorado Mesa University's Forensic Investigation Research Station (FIRS) is an enclosed outdoor research facility located on the western slope of Colorado at an elevation of 1457 m AMSL. The environment is classified as mid-latitude steppe/semi-arid cool in the Köppen–Geiger climate classification system and nets approximately 20–25 cm of precipitation annually. Human cadavers were used to study the trajectory of taphonomic change throughout the PMI.

Cadavers

Four human cadavers (A, B, C, and D) were obtained through the FIRS donor program. All cadavers underwent FIRS standard intake procedure, including review of the submitted biodemography and on-site gross assessment of perimortem height, weight, medical intervention, pathology, and trauma. Autopsied cadavers, amputees, cadavers presenting traumatic or pathological tissue change, and those in a state of active decomposition were excluded from the sample. Variables such as age, sex, ancestry, and stature were not considered exclusionary in sample selection, as these variables are often unknown in practical application.

BIA Equipment and Measurements

A Quantum IV Bioelectrical Impedance Analyzer (RJL Systems; Clinton Township, MI) was used to measure R (Ω) and X_c (Ω), using 50 kHz and 400 μA. Electrical currents were applied to the cadaver using conductive gel pad electrodes (RJL systems; Clinton Township, MI) adhered to the epidermis. To maintain electrode attachment for the duration of the study, the edges of the gel pads were glued to the epidermis, sewn in place using stitches on the corners (cadaver D only) and a duct tape cover protected the attachment areas from the environment.

The impedance measurements were carried out on each cadaver between the right hand and the right foot. The current source electrodes were positioned distally with one electrode attached to the dorsal side of the third metacarpophalangeal joint and the second electrode attached to the ventral side of the third metatarsophalangeal joint. The voltage-detecting electrodes were attached proximal to the current source electrodes (9 cm apart) with one electrode attached to the dorsal side of the radiocarpal joint and the second electrode attached to the ventral side of the talocrural articulation. The cadavers were placed in a supine

position at ground surface level within the outdoor facility with direct exposure to the elements (i.e., clothing, shade, artificial protection from elements were eliminated) for the duration of the study. Measurements were collected at regular intervals; in addition to R and X_c, ambient and local cadaver surface temperature were measured. One measurement per day was collected for each cadaver. Variables with the potential to disrupt current conduction (e.g., water/snow pooled on cadavers following rain, maggot activity in the area of electrode position) were noted and considered in analysis.

ADD

Hourly ambient temperatures were measured using an Onset HOBO remote logging weather station situated within the research facility (Onset; Bourne, MA). ADD was calculated by summing the daily mean temperatures (°C) for the study period, using a base temperature of 0°C following Vass et al. (13) and Megyesi et al. (14).

Statistical Analysis

Z (Ω) was calculated from the R and X_c measurements using the equation $Z = (R^2 + X_c^2)^{0.5}$ and standardized by stature (height; cm), $Z_H = Z/\text{stature}$. Quadratic regression was used to determine the relationship between ADD and Z. Each cadaver was analyzed individually to account for the effect of temperature on Z. The quadratic regression model was $Z_H = \beta_0 + \beta_1 \cdot \text{ADD} + \beta_2 \cdot \text{ADD}^2 + \varepsilon$. Statistical significance was determined using $\alpha = 0.05$. SigmaPlot version 13.0 (Systat Software, San Jose, CA) was used for data analysis and figure construction.

Results

Cadaver A was placed during early fall and yielded R and X_c measurements for 17 days postmortem for a maximum of 227 ADD. Cadaver B was placed during late winter and yielded measurements of R and X_c for 32 days postmortem for a maximum of 167 ADD. Cadaver C was placed during late winter and yielded measurements of R and X_c for 30 days postmortem for a maximum of 151 ADD. Cadaver D was placed during late summer and yielded measurements of R and X_c for 10 days postmortem for a maximum of 218 ADD.

All four cadavers showed a parabolic relationship between Z_H and ADD (Fig. 1). All four cadavers exhibited a statistically significant relationship between Z_H and ADD based on quadratic regressions, each with coefficients of determination >0.65 (Table 1).

Discussion

This study hypothesized that cadaver decomposition would change the configuration of the RC circuit in quantifiable ways and that BIA could be used to measure these changes. This hypothesis was supported by the statistically significant quadratic relationships observed between ADD and Z_H for all four cadavers evaluated. The relationship between ADD and Z_H was likely due to the timing of the processes identified that influence the electrical measurements of R and X_c, including postmortem changes in: the extracellular fluid ion concentration (e.g., increases in potassium concentration, total solute concentration, and osmolality) (26), extracellular fluid volume, and the decrease in intact cellular membranes (affecting both potentials for capacitive reactance and resulting in changes to physical dimensions of

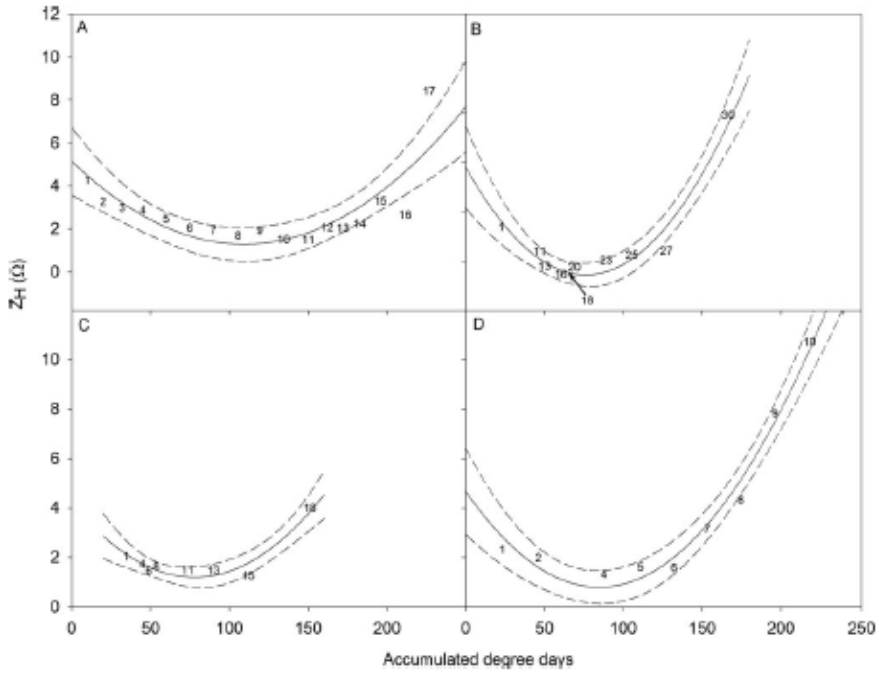

FIG. 1—*Relationship between Z_H and ADD for cadavers. The numeric value of the symbols represents the PMI in days. Quadratic regressions were used to fit solid lines. Dashed lines represent 95% confidence limits.*

TABLE 1—*Coefficients for the quadratic regression equation* $Z_H = \beta_0 + \beta_1 \cdot ADD + \beta_2 \cdot ADD^2 + \varepsilon$ *for each donor. Coefficient standard errors (SE) are in parentheses.*

Cadaver	β_0 (SE)	β_1 (SE)	β_2 (SE)	Degrees of freedom	*F*-statistic	*P*-value	Coefficient of determination (R^2)
A	5.1451 (0.7324)	−0.0706 (0.0148)	0.0003 (0.0001)	3, 14	14.331	<0.001	0.67
B	5.7973 (0.6986)	−0.1142 (0.0166)	0.0007 (0.0001)	3, 7	67.996	<0.001	0.95
C	4.1960 (0.6257)	−0.0770 (0.0159)	0.0005 (0.0001)	3, 5	27.440	0.002	0.92
D	4.6621 (0.7086)	−0.0913 (0.0132)	0.0005 (0.0001)	3, 9	127.988	<0.001	0.98

tissue). The initial decrease in Z_H was likely due to an increase in the ion concentration and the increase in the volume of extracellular fluid attendant to autolysis. The later stage increase in Z_H was likely due to progressive desiccation of the tissues or loss of the conductive fluids and the loss of capacitors (i.e., cell membranes). Similarly, Querido (25) found a significant relationship between PMI and *Z* in excised rat abdomens. Morse (27) used female rats to demonstrate the sensitivity of X_c for detecting internal hemorrhaging and blood aggregation. Mao et al. applied bioelectric impedance spectroscopy to assess bruising vitality and wound age in rat spleens (28,29), and pulmonary markers for drowning in rabbits (30). Both studies found a negative correlation between PMI and *Z* in the respective tissue mediums.

The time period that BIA measurements were possible ranged from 10 to 32 days for the four cadavers. This variation was likely due to the differences in season of placement and the variation in environmental conditions associated with each season, and the superficial placement of the gel pad electrodes. Ambient temperature plays an important role in the application of BIA. This role was evident when comparing the relationship between PMI and ADD. BIA measurements on cadavers A and D (late summer and fall placement) lasted <20 days PMI with <200 ADD. In comparison, BIA measurements on cadavers B and C (late winter placement) lasted >30 days PMI with >200 ADD. Within the cadaver, multiple variables have the potential to affect the BIA measurement period including differences in proximate body composition among cadavers and physiostructural differences (e.g., *in vivo* (perimortem) structural integrity of connective tissue, physical dimensions of cell and tissue structures and integrity of proximate adherence, osmolality, ion content and concentration, hydration, lipid aggregation, and rate and timing of tissue-specific and individual-specific autolysis). The superficial placement of gel pad electrodes results in the skin contributing to *Z* measurement. The protective barrier function of skin has the potential to reduce the length of time BIA measurements were possible. The postdeposition environment at FIRS is hot and arid, promoting rapid desiccation; this may account for the time period over which measurements were possible as water loss in superficial dermal layers occurs relatively quickly due to low overall water content and more direct exposure to the environment.

This study was the first step in developing BIA as a technique for estimating the PMI by showing a statistically significant relationship between Z_H and ADD. As this study was the first step, there are limitations present that need to be addressed in subsequent research including the parabolic relationship between Z_H and ADD, and the effects of temperature on BIA measurements. The quadratic regression models reported were not intended for application at this point. Subsequent research will inform the development of statistical models for using BIA measurements to estimate PMI. Potential avenues for future refinement of BIA include the use of multiple predictors, such as a qualitative characterization of the cadavers based on gross morphological appearance to act as a linear predictor in addition to BIA measurements. Alternate methods of attaching the electrodes may extend the time of the BIA readings. Both these refinements could change the parabolic nature of the initial data presented here and enable the development of a regression model from the BIA data collected from cadavers with known PMI. The fully developed model could then be applied to cadavers with unknown PMI to estimate the PMI of the individual.

Conclusion

The initial work on cadavers in this study and other nonhuman vertebrates demonstrate that BIA has the potential to be a powerful tool for estimating PMI. Ultimately, this technique may provide a more quantitative and less subjective approach for predicting PMI in cadavers, particularly in the later stages of decomposition. Further research is necessary to understand areas for improving the technique and for developing predictive models.

Acknowledgments

The authors wish to thank the donors and their families, without whom this research would not be possible. The students and technicians that assisted with donor placement and data collection. This project includes both data collected prior to a National Institute of Justice grant (2015-DNBX-K015) and statistical analyses and publication completed under the auspices of the grant.

References

1. Cantürk I, Çelik S, Şahin MF, Yağmur F, Kara S, Karabiber F. Investigation of opacity development in the human eye for estimation of the postmortem interval. Biocybern Biomed Eng 2017;37(3):559–65.
2. Chandrakanth HV, Kanchan T, Balaraj BM, Virupaksha HS, Chandrashekar TN. Postmortem vitreous chemistry – an evaluation of sodium, potassium and chloride levels in estimation of time since death (during the first 36 h after death). J Forensic Legal Med 2013;20(4):211–6.
3. Gulyás B, Dobai JJ, Szilágyi G, Csécsei G, Székely GJ. Continuous monitoring of post mortem temperature changes in the human brain. Neurochem Res 2006;31(2):157–66.
4. Henssge C, Althaus L, Bolt J, Freilederer A, Haffner HT, Henssge CA, et al. Experiences with a compound method for estimating the time since death. I. Rectal temperature nomogram for time since death. Int J Legal Med 2000;113(6):303–19.
5. Baccino E, De Saint Martin L, Schulier Y, Guilloteau P, LeRhun M, Morin JF, et al. Outer ear temperature and time of death. Forensic Sci Int 1996;83(2):133–46.
6. Kaliszan M, Hauser R, Buczyn′ ski J, Raczyn′ ska K, Jankowski Z, Kernbach-Wighton G. The potential use of the eye temperature decrease in determining of the time of death in the early post-mortem period studies in pigs. Am J Forensic Med Pathol 2010;31(2):162–4.
7. Usumoto Y, Hikiji W, Sameshima N, Kudo K, Tsuji A, Ikeda N. Estimation of postmortem interval based on the spectrophotometric analysis of postmortem lividity. Legal Med 2010;12(1):19–22.
8. Kaliszan M, Hauser R, Kernbach-Wighton G. Estimation of the time of death based on the assessment of post mortem processes with emphasis on body cooling. Legal Med 2009;11(3):111–7.

9. Wyler D, Marty W, Bär W. Correlation between the post-mortem cell content of cerebrospinal fluid and time of death. Int J Legal Med 1994;106(4):194–9.
10. Gos T, Raszeja S. Postmortem activity of lactate and malate dehydrogenase in human liver in relation to time after death. Int J Legal Med 1993;106(1):25–9.
11. DiMaio VJ, DiMaio D. Time of death. In: Forensic pathology. Boca Raton, FL: CRC Press LCC, 2001;21–42.
12. Vass AA. The elusive postmortem interval formula. Forensic Sci Int 2011;204(1–3):34–40.
13. Vass AA, Bass WM, Wolt JD, Foss JE, Ammons JT. Time since death determinations of human cadavers using soil solution. J Forensic Sci 1992;37(5):1236–53.
14. Megyesi MS, Nawrocki SP, Haskell NH. Using accumulated degree-days to estimate the postmortem interval from decomposed human remains. J Forensic Sci 2005;50(3):618–26.
15. Dabbs GR. Caution! All data are not created equal: the hazards of using National Weather Service data for calculating accumulated degree days. Forensic Sci Int 2010;202(1–3):e49–52.
16. Dabbs GR. How should forensic anthropologists correct national weather service temperature data for use in estimating the postmortem interval? J Forensic Sci 2015;60(3):581–7.
17. Metcalf JL, Xu Z, Boulsimani A, Dorrestein P, Knight R. Microbiome tools for forensic science. Trends Biotechnol 2017;35(9):814–23.
18. Finley SJ, Benbowb ME, Javan GT. Potential applications of soil microbial ecology and next-generation sequencing in criminal investigations. Appl Soil Ecol 2015;88:69–78.
19. Hoffer EC, Meador CK, Simpson DC. Correlation of whole-body impedance with total body water volume. J Appl Physiol 1969;27(4):531–4.
20. Kyle UG, Bosaeus I, De Lorenzo AD, Deurenberg P, Elia M, Gomez JM, et al. Bioelectrical impedance analysis – part I: review of principles and methods. Clin Nutr 2004;23(5):1226–43.
21. Gabriel C, Gabriel S, Corthout E. The dielectric properties of biological tissues: I. Literature survey. Phys Med Biol 1996;41(11):2231–49.
22. Van Marken Lichtenbelt WD. The use of bioelectrical impedance analysis (BIA) for estimation of body composition. In: Speakman JR, editor. Body composition analysis of animals: a handbook of non-destructive methods. Cambridge, U.K.: Cambridge University Press, 2001;161–87.
23. Querido D. Temperature-correction of abdominal impedance: improved relationship between impedance and postmortem interval. Forensic Sci Int 2000;109(1):39–50.
24. Querido D. Preliminary study of the effect of acute antemortem haemorrhage on postmortem abdominal impedance in rats. Forensic Sci Int 2002;127(3):218–24.
25. Querido D. Postmortem changes in electrical resistance of the gastric wall during the early postmortem period in rats. Forensic Sci Int 1992;53 (1):81–92.
26. Querido D. Postmortem changes in resistivity of the anterior abdominal wall during the early postmortem period in rats. Forensic Sci Int 1993;60 (3):163–77.
27. Morse J. Electrical bioimpedance as a detection tool for internal hemorrhaging and blood aggregation [thesis]. Ottawa, Canada: University of Ottawa, 2014.
28. Mao S, Dong X, Fu F, Seese RR, Wang Z. Estimation of postmortem interval using an electric impedance spectroscopy technique: a preliminary study. Sci Justice 2011;51(3):135–8.
29. Mao S, Fu F, Dong X, Wang Z. Supplementary pathway for vitality of wounds and wound age estimation in bruises using the electric impedance spectroscopy technique. J Forensic Sci 2011;56(4):925–9.
30. Mao S, Fu F, Dong X, Seese RR, Wang Z. A contributory diagnosis of drowning in putrefactive corpses using the electric impedance spectroscopy. Rom J Leg Med 2010;18(4):283–8.

Additional information and reprint requests:
Eriek S. Hansen, Ph.D.
Department of Biological Sciences
Colorado Mesa University
1100 North Avenue
Grand Junction
CO 81501
E-mail: erihansen@coloradomesa.edu

JOURNAL OF FORENSIC SCIENCES

J Forensic Sci, 2017
doi: 10.1111/1556-4029.13727
Available online at: onlinelibrary.wiley.com

PAPER

ANTHROPOLOGY

Melissa Connor,[1] Ph.D.; Christiane Baigent,[1] M.Sc.; and Eriek S. Hansen,[2] Ph.D.

Testing the Use of Pigs as Human Proxies in Decomposition Studies*

ABSTRACT: Pigs are a common human analogue in taphonomic study, yet data comparing the trajectory of decomposition between the two groups are lacking. This study compared decomposition rate and gross tissue change in 17 pigs and 22 human remains placed in the Forensic Investigation Research Station in western Colorado between 2012 and 2015. Accumulated degree days (ADD) were used to assess the number of thermal units required to reach a given total body score (TBS) (1) which was used as the measure of decomposition. A comparison of slopes in linear mixed effects model indicated that decomposition rates significantly differed between human donors and pig remains $\chi^2_{(1)} = 5.662$, $p = 0.017$. Neither the pig nor the human trajectory compared well to the TBS model. Thus, (i) pigs are not an adequate proxy for human decomposition studies, and (ii) in the semiarid environment of western Colorado, there is a need to develop a regional decomposition model.

KEYWORDS: forensic science, taphonomy, decomposition, animal models, human proxies

Interest in forensic taphonomy has increased steadily over the last forty years. The interaction between human remains and the postdeposition environment may alter or obscure features necessary for effective analysis of postmortem interval (PMI), trauma, pathology, and the biological profile, affecting the analytical conclusions and the quality of information gained. Facilities with the capacity to study human remains increased from one facility in 1981 to seven facilities worldwide in 2017. Due to anatomical and physiological similarities to humans, pigs (*Sus scrofa*) are a standard proxy for those endeavoring to study taphonomy outside of these facilities. Similarities between pigs and humans frequently cited as the basis for equivalence include: internal anatomy, diet, endogenous microbiome, fat-to-muscle ratio, tissue density, structure, density, and distribution of body hair, monogastric digestive system, and omnivorous diet (2). Due largely to cost and ability to amass large sample sizes, smaller animals, such as rabbits, are also frequently used (3). However, aside from identifying general overlap in anatomy and physiology, the efficacy of the use of pigs as human analogues remains largely untested.

The origin of pigs as human proxy can primarily be traced to entomological studies where the use of animal proxies for the comparison of insect succession throughout decomposition is well tested. Rodriguez and Bass (4) compared available insect succession data collected from canine cadavers (5) to that observed on human cadavers and found significant overlap. It appears that the majority of insect species (99.67%) show no preference between pigs or humans (6,7). However, caution is warranted when using entomological studies to validate the use of pig carrion in decomposition studies. While the entomologist and anthropologist both seek to understand PMI, it is incorrect to assume that the disciplines are studying the same underlying physiological phenomenon. The entomologist is concerned with insect development, progression, and succession guided by the sum of the decomposition event (e.g., the release of chemical constituents that guide chemotaxis, moisture content and related patterns of oviposition, and visual and mechanosensory cues that govern insect movement). Conversely, the anthropologist is concerned with the sum of stages of gross morphological change, which may correlate with various stages of decomposition (e.g., rate, chronology, and presentation of tissue dissolution under various circumstances). Therefore, the biological features that make pigs a viable research tool in entomology cannot be assumed to translate to taphonomic investigation.

Early observational studies on decomposition used a variety of species, including cows, seabirds, and sea mammals (8). Payne (9) studied dogs, cats, squirrels, rabbits, chickens, birds, and pigs, concluding that relatively large animals of uniform size were best for his studies (10). The results of these studies were rarely compatible and consistently resulted in opposing criteria and sequences used to describe the trajectory of decomposition. Micozzi (10) suggested that the incompatibility was due to the wide variety of animals used and the conditions under which the studies were carried out. Stokes et al. (11) evaluated potential proxies for use in soil decomposition studies. A suite of physiochemical soil characteristics was compared among and between tissue types using small samples of skeletal muscle tissue from humans, pork, beef, and lamb. Different species exhibited similar patterns of change, but none of the proxies were an ideal predictor of human skeletal muscle tissue for soil decomposition studies. Wang et al. (12) conducted a comparative analysis of insect

[1]Forensic Investigation Research Station, Colorado Mesa University, 1100 North Ave, Grand Junction, CO 81506.
[2]Department of Biological Sciences, Forensic Investigation Research Station, Colorado Mesa University, 1100 North Avenue Grand Junction, Grand Junction, CO 81501-7611.

*Presented in part at the 68th Annual Scientific Meeting of the American Academy of Forensic Sciences, February 22-27 2016, in Las Vegas, NV.

Received 27 Oct. 2017; and in revised form 7 Dec. 2017; accepted 8 Dec. 2017.

succession on human remains, pig carrion comprising two size categories, and rabbit carrion. They conclude that body size and decomposition rate share an inverse relationship, and insect species diversity and complexity are more complicated on larger remains. Dipteran development rate was consistent across all size and species categories, although a subset of forensically significant Calliphoridae species were unable to complete first-generation development on rabbit carrion. Dautartis et al. (13) observed a similar correlation between body size and trajectory of decomposition. Five each of pigs, humans, and rabbits were used to study gross morphological changes and insect activity across a 5-month interval. The conclusion was that the pattern of decomposition differed between the three groups, and they were not likely to be interchangeable for decomposition research. However, the continuing challenge in using human remains for research study is sample size. While these studies present intriguing patterns, there is still a need for research conducted within human samples, using larger sample sizes, and in differing environments. Additionally, longitudinal studies are warranted in dry areas where desiccation occurs and bodies take much longer than 5 months to skeletonize. The goal of this research was to further test whether, and to what degree, pigs provide a useful proxy for human decomposition.

Materials and Methods

Observations were made at the Forensic Investigation Research Station (FIRS), Colorado Mesa University, located on the western slope of Colorado. The FIRS performs ongoing research using human donors to study the trajectory of taphonomic change. The FIRS is situated at an elevation of 1457 m AMSL. The environment is classified as mid-latitude steppe/semiarid cool in the Köppen–Geiger climate classification system and nets approximately 20–25 cm of precipitation annually. Five years of on-site data collection yields an average high of 33.33°C with daily highs exceeding 41.1°C and an average low of −3.88°C, with daily lows exceeding −25.27°C. The western slope is a relatively sunny area, receiving approximately 70% of available sunshine. The FIRS is in the area of Utaline-Neiman-Lazear association of soils. These are well-drained loam soils formed in materials weathered from basalt and sandstone (14). The county soil map shows that the facility is in an area of Billings silty clay loam (14). The natural vegetation is primarily four-winged saltbush (*Atriplex canescens*), rabbitbrush (*Ericameria nauseosa*), galleta (*Pleuraphis jamesii*), and Indian rice grass (*Achnatherum hymenoides*).

This study compared the pattern of decomposition in 17 pig carrion and 22 human remains. Animal and human remains were placed in the facility between September 2012 and December 2015. The pigs were systematically placed so that the first 12 were placed one pig a month from September 2012 to August 2013. The remaining five pigs were placed on the same day as our second through sixth human bodies. The human remains were placed when they were received as part of FIRS donation program, resulting in placement during all four seasons. The numbers of human remains placed each month were: January=3; February=3; March=2; May=2; July=2; August=2; September=2; October=2; November=2; December=2. Although a convenience sample, the sample represents all seasons.

Hourly environmental data were collected from an Onset HOBO remote-logging weather station placed within the research facility (Onset; Bourne, MA). Accumulated degree days (ADD) were used as an indice of PMI and calculated using a base temperature of 0°C following Vass et al. (15) and Megyesi et al. (1). Decomposition was scored at regular intervals following Megyesi et al.'s (1) total body score (TBS) system. The ADD was calculated for each date that a TBS score was collected, resulting in 2627 ADD-TBS pairs for the human subjects and 1100 ADD-TBS pairs for the pig subjects.

Euthanized pigs were delivered to FIRS for placement within less than four hours of death; the supplier euthanized the pigs with a gunshot wound to the head. Body sizes ranged between 25 and 64 kg at the time of death, with a median of 35 kg. Both male and female pigs were included in this study. A single supplier was used, and the pigs were fed similar diets, lived in a similar environment, and were in generally good health at the time of euthanization. None of the pigs were refrigerated. The initial TBS for all pig subjects was three.

The human sample was amassed under the auspices of the FIRS human donation program. Cause of death within the human sample included pathogeneses summarily categorized as "natural" (e.g., heart attack), diagnosed chronopathology (e.g., cancer, lupus), and trauma (blunt force following a fall). Because the thoracoabdominal incision attendant to autopsy approximates dramatic penetrating trauma, and the trajectory of decomposition in autopsied versus nonautopsied remains has not yet been assessed at FIRS, autopsied remains were excluded from this study. Intragroup rate and pattern of decomposition were also considered. Placement of human remains varied from the day of death with no refrigeration prior to placement to 53 days postmortem with refrigeration in the interim. If date of death was unknown, donors presenting a TBS >7 (fresh to early decomposition on the Megyesi scale) were excluded from this study. Pig and human remains were photographed and scored at regular intervals consistent with FIRS TBS protocols (16). Under the data collection protocol, each body was scored daily until a TBS of 24 was reached. To allow for visible changes to accrue (i.e., score-able changes), remains with TBS ≥24 were scored weekly for humans and monthly for pigs. This protocol was adhered to as weather and staffing allowed. All personnel performing data collection were trained and tested in FIRS data collection protocol prior to entering the facility, and all training scores were assessed blindly by two full-time staff members to ensure that data quality and accuracy were maintained, and inter-observer error was minimal. Individual remains were not caged as scavenging was infrequent and limited to small areas of soft tissue loss.

The decomposition rates of the pigs and humans were compared using two methods. For the first comparison, the mean, median, and coefficient of variation of ADD were calculated for each TBS point and visually assessed (Table 1, Figs 1–3). Additionally, a linear mixed model (LMM) using maximum likelihood estimates was used to determine if decomposition rate varied between the human and pig groups. The use of LMM was advantageous to account for unbalanced design and repeated measurements on single remains, which has the potential to highlight both inter- and intra-sample variation. In the LMM, the dependent variable was TBS (TBS^2 transformation). The independent fixed variables were ADD (Log_{10} (ADD+1) transformation), an indicator variable for human (indicator = 1) or pig (indicator = 0) remains, and an interaction term (Log_{10}(ADD+1) x Indicator). The random effects for both intercepts and slopes were ADD and the individual remains. The interaction term was used to test for a statistical difference between slopes. The *p*-value for the interaction was determined by a likelihood test comparing the models with and without the interaction term.

TABLE 1—*The mean and coefficient of variation of ADD at each TBS point for humans and pigs. "N/A" indicates that no specimens were scored at that TBS interval.*

TBS	Pig ADD	Pig Coefficient of Variation	Human ADD	Human Coefficient of Variation
3	9.42	109.74	11.43	100.28
4	N/A	N/A	8.74	122.98
5	15.32	92.30	25.57	75.83
6	27.42	70.57	23.26	86.77
7	31.19	50.08	15.18	84.57
8	47.38	53.52	39.77	80.75
9	46.41	67.36	35.47	77.56
10	63.71	56.01	55.30	77.40
11	74.97	51.40	94.13	68.61
12	108.36	68.76	91.35	70.91
13	118.22	55.18	127.69	58.32
14	145.80	57.24	175.93	53.59
15	201.89	59.79	221.76	56.94
16	206.93	46.56	236.01	58.76
17	513.89	177.73	241.09	59.26
18	466.68	172.0	379.91	131.51
19	1194.82	126.38	519.92	115.21
20	993.65	131.86	594.17	83.86
21	2356.82	96.35	1296.11	92.20
22	1482.82	156.92	2081.71	68.79
23	1979.29	131.01	3175.87	63.06
24	3881.73	76.94	5218.36	59.21
25	5751.12	61.77	5614.57	58.01
26	4225.05	81.23	6042.73	60.24
27	4963.49	86.71	6711.08	59.99
28	5159.25	69.79	4711.35	46.19
29	6991.28	58.76	4501.79	27.94
30	8002.54	59.00	4543.18	18.63
31	8738.27	59.15	5270.26	5.15
32	10515.97	43.99	N/A	N/A
33	9263.33	47.18	N/A	N/A
34	9711.82	36.12	N/A	N/A
35	13246.84	27.61	N/A	N/A
36	12168.09	0.16	N/A	N/A

ADD, accumulated degree days.

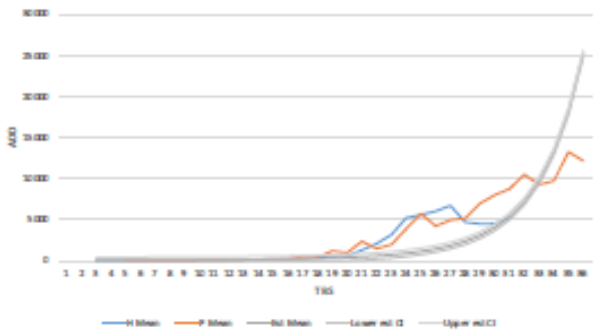

FIG. 1—*Pig and human ADD mean for each TBS score compared to the estimated ADD from the TBS model (1). ADD, accumulated degree days; TBS, total body score.*

The analysis was conducted in Program R (version 3.4.0) using the lme4 package (17,18).

Results

Visual assessment of the TBS means and coefficients of variation in pigs and humans against the model (Fig. 1) made it apparent that the data from FIRS were no longer represented by the model after a TBS of 18. The human and pig mean ADD and median ADD for each TBS point also differed with humans requiring a greater ADD to reach a specific TBS until about a TBS of about 27, and then, the pigs required a greater ADD to reach a specific TBS (Fig. 2, Table 1). A visual assessment of the coefficient of variation suggests that initially the human sample varies more than the pig in the number of ADD required to reach a specific TBS, after a TBS of approximately 15, when the pig sample generally has a greater variation (Fig. 3, Table 1).

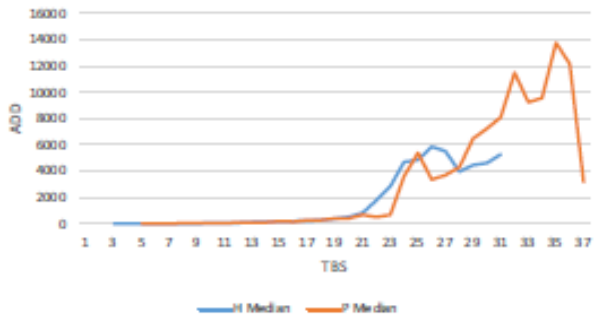

FIG. 2—*Pig and human median ADD for each TBS score. ADD, accumulated degree days; TBS, total body score.*

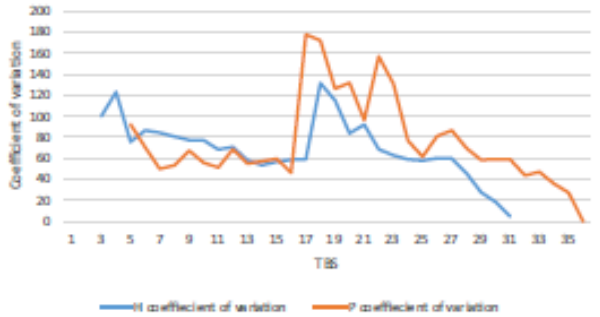

FIG. 3—*Pig and human ADD coefficient of variation for each TBS score. ADD, accumulated degree days; TBS, total body score.*

The LMM indicated that decomposition rates significantly differed between human donors and pig remains based on a comparison of slopes of the interaction coefficient $\chi^2_{(1)} = 5.662$, $p = 0.017$ (Fig. 4). The LMM model used 2626 observations for the 22 humans and 1101 observations for the 17 pigs. The LMM for the fixed effects with standard errors in parentheses was

$$\begin{aligned} \mathrm{TBS}^2 = {} & 351.59(49.55) + 304.66(21.57) \cdot \mathrm{Log}_{10}(\mathrm{ADD}{+}1) \\ & + 171.25(66.05) \cdot \mathrm{Indicator} - 85.88(28.80) \\ & \cdot \mathrm{Log}_{10}(\mathrm{ADD}{+}1) \cdot \mathrm{Indicator} \end{aligned}$$

marginal $R^2 = 0.67$ (fixed effects) and conditional $R^2 = 0.90$ (both fixed and random effects).

Discussion

In approximately 60% of the pig specimens, the intestines ruptured through the abdomen during the bloat phase (Fig. 5);

This resource was prepared by the author(s) using Federal funds provided by the U.S. Department of Justice. Opinions or points of view expressed are those of the author(s) and do not necessarily reflect the official position or policies of the U.S. Department of Justice.

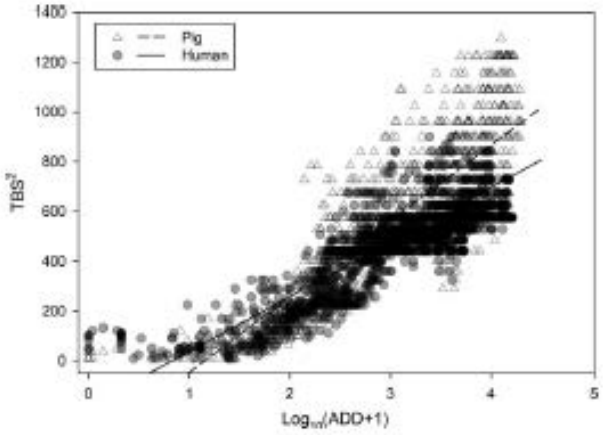

FIG. 4—*Comparison of decomposition rates between humans and pigs. Regression lines were fit using the fixed effects from the LMMs.*

FIG. 5—*Intestinal rupture in pig.*

abdominal rupture did not occur in any of the human specimens. While humans and pigs present anatomical, physiological, and genetic overlap, fundamental differences between the two species exist. While both humans and pigs are monogastric, key differences in the structure and function of the gastrointestinal tract (GIT) may affect the rate, timing, and trajectory of decomposition. On average, the human intestine (large and small) is 7.5 m in length, as opposed to 23 m in the pig. The pig small intestine further presents differences in segment length and branching of mesenteric vessels and attendant anastomoses (which facilitate cellular communication with surrounding tissues). In the human GIT, ileal Peyer's patches (PP) are an aggregate of lymphoid modules that facilitate an immune response within the mucosa by monitoring intestinal bacteria and inhibiting growth and spread of pathogenic strains. Conversely, the ileal PP in pigs is continuous, which not only constitutes a structural difference, but also implies major differences in typical bacterial load, potential exposure to pathogenic bacteria, and enteric colonization. A pyloric diverticulum—a site for microbial metabolism of ingesta—is present in pigs but absent in typical human anatomy (19). Finally, the cecum, ascending and transverse colon, and the proximal portion of the descending colon are oriented in a series of centrifugal and centripetal coils to accommodate length and orientation associated with quadrupedalism, which differ from the folded and "stacked" structure of the human intestines.

The sum of these many subtle differences may contribute dramatically to gross differences in decomposition, such as the abdominal rupture observed in this sample. In more basic terms, while this phenomenon is likely multifactorial, a significantly longer GIT summarily constitutes larger cubic volume of lumina within which decompositional gasses have the potential to aggregate, resulting in greater potential for eruptive response.

Overall similarity in TBS scores in pigs and humans in early decomposition may be an artifact of the overfitting of data to the scoring system; data collection necessitates that a score be applied so the "best choice" category regardless of overall technical accuracy. Only six categories in the head/neck and five in the trunk and limbs describe early decomposition. Limited scoring options may reduce or eliminate the resolution necessary to highlight divergence in gross change. Keogh et al. (20) used the Megyesi et al. (1) TBS to define the typical trajectory of human decomposition and compared this to observations made within a sample of 20 pig carrion. The authors concluded that the gross changes observed between the two groups were sufficiently different to warrant a separate scoring system for pig carrion. However, TBS comparison was limited to pigs and did not include humans in the sample environment, so the differences observed may be a combination of species and environment.

Total body score values for both species plateaued between 21 and 24 for an extended period of ADD. The humans plateaued in moist decomposition for a longer period of ADD. The pigs were a clinically healthy weight, while over half the human sample was overweight or obese. Body fat does impact decomposition, hindering dissipation of heat and providing liquid for bacterial growth and insect oviposition. With regard to the human sample, the presence of diabetes mellitus accelerates decomposition (21); as a strong correlation with obesity and with an estimated seven million undiagnosed cases per annum (http://www.diabetes.org/diabetes-basics/statistics/ (accessed September 30, 2017)), the unreported presence of the disease should be considered in research and in medicolegal investigation. The cause of death in the human sample included chronopathology (cancer and lupus) and traumatic injury. Antemortem infection, wounds, and chronopathology may accelerate putrefaction by inducing hyperthermia secondary to pathogenesis (including tertiary infection such as sepsis), or as the result of medication (21). Wounds also provide additional places for insect oviposition. The plateau observed among both human and pig samples is likely due to environmental factors at the FIRS. In FIRS' arid climate, remains tend to desiccate, rather than skeletonize. Dermal tissue and underlying viscera are hygroscopic in nature and therefore may be expected to react similarly to environmental conditions. Visceral retention following desiccation was noted in several human cadavers at FIRS. These phenomena have not been observed in pigs and may be the result of visceral eruption or another generalized pattern of decomposition.

Compared to the human sample, the pigs were a more superficially homogenous sample at the start of the project; control over variables such as weight, cause of death, reported pathology, and immediacy of placement within the facility reduced intragroup variation. Such a homogenous sample may allow researchers to control variables and identify trends in decomposition, but identified trends need to be validated within human samples before their efficacy can be accurately reported and extreme caution is warranted when attempting to validate a study conducted on humans within a pig sample. The use of pigs in research has the potential to complicate judicial proceedings where researchers are asked to testify on the condition of human remains based on

their knowledge of pig decomposition, or where established methods are called into question under the Daubert Standard following publication of research conducted within pig samples.

The human remains were a more variable group, but a more realistic sample of forensic cases. Because forensic cases often involve unknown circumstance, the variation among the human sample was in fact reflective of the variation that any useful decomposition measure must encompass to provide an estimate of the PMI. In this sense, discerning patterns among homogenous proxy populations may provide a false sense that the same conclusions are applicable to a much less homogenous population. Forensic disciplines are still attempting to understand how the interaction of complex variables affects human decomposition—a conservative approach is critical when drawing direct correlations between humans and proxies.

The initial samples of pigs appear more homogenous and humans more varied, but the pigs tend to have a greater coefficient of variation (Table 1, Figs 3, 4), particularly after a TBS of 25. This may partly be due to the fact that the TBS model was created for humans and does not work as well with pigs (20). Furthermore, while a pig sample may present as "healthy" and homogeneous in gross examination, animals reared for consumption are not subject to regular health assessment and should not be assumed to be homogeneously "healthy" at the time of death. Pathological stimulants identified in research include immunocompromise following psychosocial stress, including decreased antibody response to antigenic challenge relative to stock density (22) and increases in viral–bacterial load, such as *Salmonella* following exacerbated norepinephrine excretion which Bearson and Bearson (23) demonstrated may directly impact growth and virulence of *Salmonella*, including the upregulation of genes resulting in enhanced motility. Disease associated with commercial rearing, captivity, and confinement is sufficient to result in research dedicated to locating ever emerging biomarkers for pig disease in an effort to curb economic loss (24). The exercise here was not to provide a comprehensive cross section of pig pathology, but to demonstrate that gross examination and meeting variables dictated by sample requirements are not a sufficient means for determining "health" in a biologically diverse species which has demonstrated strong immunosensitivity to the antemortem environment. The sum of the anatomical, physiological, and pathological differences presented may be manifest in unexpected ways at any time throughout the decomposition event. As researchers struggle to understand the diverse complexity of human decomposition, it is specious to suggest that the intersection of captivity, dynamic zoonotic disease processes, death, and decomposition may be overlooked and a distinct and diverse species defined as homogenous to meet analytical needs.

Finally, the TBS model used by many decomposition studies does not work well with pigs and, for the data presented, fit neither pig nor human data in late-stage decomposition. This was likely due to the desiccation seen in FIRS' semi-arid environment and highlights the need for region-specific validation of models used to estimate postmortem interval.

Conclusion

When compared using the TBS model, the trajectory of decomposition observed between human and pig samples diverged in rate and gross presentation. Additionally, the TBS scoring model did not perform well in the arid environment at the FIRS. Regional decomposition patterns may require regional scoring models. Nonhuman proxies do provide a superficially homogenous sample allowing isolation of individual variables and have the potential to indicate trends in taphonomy. Human samples tend to be more variable, particularly in body composition and cause of death, both of which affect the pattern of decomposition. Pigs may be useful in studying general trends. However, they are not a substitute for human subjects, and caution is warranted when attempting to apply data derived from pigs to human subjects, especially in medicolegal investigation. Above all, reliance on a relatively homogenous proxy sample may make researchers overconfident in their ability to predict the timing and patterns of decomposition.

Acknowledgments

The authors wish to thank the donors and their families, without whom this research would not be possible. The students and technicians that assisted with donor placement and data collection. Sara Garcia helped with editing, and numerous FIRS interns collected data that used in this project.

References

1. Megyesi M, Nawrocki SP, Haskell NH. Using accumulated degree-days to estimate the postmortem interval from decomposed human remains. J Forensic Sci 2005;5(3):618–26.
2. Palosh CM, Rogers TL. Tissue decomposition of submerged, dismembered pig limbs enclosed in plastic. J Forensic Sci 2009;54(6):1223–8.
3. Troutman L, Moffatt C, Simmons TA. Preliminary examination of differential decomposition patterns in mass graves. J Forensic Sci 2014;59(3):621–6.
4. Rodriguez WC, Bass WM. Insect activity and its relationship to decay rates of human cadavers in east Tennessee. J Forensic Sci 1983;28(2):423–32.
5. Reed HB. A study of dog carcass communities in Tennessee with special reference to insects. Am Midl Nat 1958;59:213–45.
6. Schoenly KG, Haskell NH, Hall RD, Gbur JR. Comparative performance and complementarity of four sampling methods and arthropod preference tests from human and porcine remains at the forensic anthropology center in Knoxville, Tennessee. J Med Entomol 2007;44:881–94.
7. Haskell NH, Schoenly K, Hall RD. Testing reliability of animal models in research and training programs in forensic entomology, part II, final report. Washington, DC: U.S. Department of Justice, National Criminal Justice Reference Service (NCJRS), 2002.
8. Shafer W. The ecology and paleoecology of marine environments. Chicago, IL: University of Chicago Press, 1978.
9. Payne JS. A summer carrion study of the baby pig Sus Scrofa Linnaeus. Ecology 1965;46(5):592–602.
10. Micozzi MS. Postmortem change in human and animal remains: a systematic approach. Springfield, IL: Charles C. Thomas, 1991.
11. Stokes KL, Forbes SL, Tibbett M. Human versus animal: contrasting decomposition dynamics of mammalian analogues in experimental taphonomy. J Forensic Sci 2013;58(3):583–91.
12. Wang L, Wang Y, Li L, Wang J, Wang M, Zhang Y, et al. Temperature-dependent development of parasarcophaga similis (Meade 1876) and its significance in estimating postmortem interval. J Forensic Sci 2017;62(5):1234–43.
13. Dautartas AM, Jantz LM, Vidoli GM, Steadman DW. A multidisciplinary validation study of non-human animal models for decomposition research: a time series approach. Proceedings of the 67th Annual Scientific Meeting of the American Academy of Forensic Sciences; 2015 Feb 16-21; Orlando, FL. Colorado Springs, CO: American Academy of Forensic Sciences, 2015.
14. Spears CF, Kleven EV. Soil survey of Mesa County area, Colorado. Washington, DC/Fort Collins, CO: Soil Conservation Service and Colorado Agricultural Experiment Station, 1978.
15. Vass AA, Bass WM, Wolt JD, Foss JE, Ammons JT. Time since death determinations of human cadavers using soil solution. J Forensic Sci 1992;37(5):1236–53.

16. Baigent CA, editor. TBS and photography protocol. Forensic Investigation Research Station. Connor M, series editor. FIRS Technical Report Series #2. Grand Junction, CO: Colorado Mesa University, 2017.
17. Bates D, Maechler M, Bolker B, Walker S. Fitting linear mixed-effects models using lme4. J Stat Softw 2015;67(1):1–48.
18. R Core Team. R: A language and environment for statistical computing. Vienna, Austria: R Foundation for Statistical Computing, 2017; https://www.R-project.org/ (accessed September 30, 2017).
19. Meurens F, Summerfield A, Nauwynck H, Saif L, Gerdts V. The pig: a model for human infectious diseases. Trends Microbiol 2012;20(1):50–7.
20. Keogh N, Myburgh J, Steyn M. Scoring of decomposition: a proposed amendment to the method when using a pig model for human students. J Forensic Sci 2017;62(4):986–93.
21. Zhou C, Byard R. Factors processes causing accelerated decomposition in human cadavers – an overview. J Forensic Leg Med 2011;18(1):6–9.
22. Proudfoot K, Habing G. Social stress as a cause of diseases in farm animals: current knowledge and future directions. Vet J 2015;206(1):15–21.
23. Bearson BL, Bearson SM. The role of the QseC quorum-sensing sensor kinase in colonization and norepinephrine-enhanced motility of Salmonella enterica serovar Typhimurium. Microb Pathog 2008;44(4):271–8.
24. Giles TA, Belkhiri A, Barrow PA, Foster N. Molecular approaches to the diagnosis and monitoring of production diseases in pigs. Res Vet Sci 2017;114:266–72.

Additional information and reprint requests:
Melissa Connor, Ph.D.
Forensic Investigation Research Station
Colorado Mesa University
1100 North Ave
Grand Junction
CO 81506
E-mail: mconnor@coloradomesa.edu